Future flood envelope curves for the estimation of design flood magnitudes for highway bridges

Dona Maria

Department of Civil Engineering, McGill University, Montreal

March 2024

A thesis submitted to McGill University in partial fulfillment of the requirements of the degree of Master of Science

ABSTRACT

The rising costs and safety concerns associated with flood-related infrastructure damages in Canada underscores the critical need for adapting design flood magnitudes to future climate change. Creager flood envelope curves, which serve as the upper bound/limit of observed extreme flows for different drainage areas for a given region, are commonly used by practitioners to estimate design flood magnitudes, which in the case of most river-crossing highway bridges is considered as 75-year flood magnitude. This study proposes a framework for adapting Creager curves to future changes in streamflow. To this end, Creager curves, for the current 1951–2020 period, are developed considering 417 observation stations, located in seven major Canadian river basins (i.e., Fraser, Nelson, Mackenzie, Yukon, Churchill, St Lawrence and St John), using regional frequency analysis (RFA). The Creager coefficient C, which is the main parameter that defines flood envelope curves for different regions, for current climate, exhibits considerable variability, ranging from 1 to 45, across the studied river basins. To adapt Creager curves for future changes, a correction factor, R_C, which is the ratio of future to current period C values is proposed. This is obtained for the observation sites, using simulated streamflow data, derived using a cell-to-cell routing scheme, applied to an ensemble of five-member Regional Climate Model (RCM) GEM (Global Environmental Multiscale) simulated runoff for the current reference 1951–2020 and future 2021–2099 periods, through two RFA approaches. The first RFA approach, considering only the GEM cells where the stations are located, suggests R_C in the 0.3 to 1.6 range, with St John and St Lawrence River basins showing R_C values less than 1. An evaluation of the level of confidence for R_C, based on the GEM ensemble, reveal a higher level of confidence for most parts of the study domain. The second approach, considering all GEM cells for a given region, yields a wider range for R_C and adds useful information in that R_C values can also be established at

ungauged locations. The second approach is likely to be a better choice for longer return periods considering the larger pooling of data. From a practical viewpoint, the proposed method for estimating future design floods is robust and transferrable to other basins but can benefit from using streamflow projections from other models for better quantification of uncertainty.

RESUME

L'augmentation des coûts et les préoccupations en matière de sécurité associées aux dommages aux infrastructures liés aux inondations au Canada soulignent la nécessité d'adapter les magnitudes de crue utilisées dans la conception aux changements climatiques futurs. Les courbes d'enveloppe de crue de Creager, qui servent de limite supérieure des débits observés pour différents bassins versants d'une région donnée, sont couramment utilisées par les praticiens pour estimer la magnitude des crues, ce qui, dans le cas de la plupart des ponts routiers traversant des rivières, correspond à une magnitude de crue sur 75 ans. Cette étude propose un cadre pour adapter les courbes de Creager aux changements futurs du débit. À cette fin, les courbes de Creager, pour la période actuelle 1951-2020, sont élaborées en considérant 417 stations d'observation, situées dans sept grands bassins fluviaux canadiens (c.-à-d. Fraser, Nelson, Mackenzie, Yukon, Churchill, Saint-Laurent et Saint-Jean), en utilisant une analyse de fréquence régionale. Le coefficient de Creager C, qui est le principal paramètre qui définit les courbes d'enveloppe des crues pour différentes régions, présente une variabilité considérable, allant de 1 à 45, à travers les bassins fluviaux étudiés, pour le climat actuel. Pour adapter les courbes de Creager aux changements futurs, un facteur de correction, R_C, qui est le rapport entre les valeurs C pour les période future et actuelle, est proposé. Ceci est obtenu pour les sites d'observation en utilisant des débits simulés, dérivés à l'aide d'un schéma de routage de cellule à cellule, appliqué à un ensemble de cinq membres des simulations du modèle climatique régional GEM (Global Environmental Multiscale) pour la période de référence actuelle 1951-2020 et la période future 2021-2099, à travers deux approches dans l'analyse de fréquence régionale. La première approche, considérant uniquement les cellules GEM où sont situées les stations, suggère un R_C compris entre 0.3 et 1.6, les bassins du Saint-Jean et du Saint-Laurent affichant des valeurs R_C inférieures à 1. Une évaluation du

niveau de confiance pour R_C, basés sur l'ensemble GEM, révèlent un niveau de confiance plus élevé pour la plupart des parties du domaine d'étude. La deuxième approche, prenant en compte toutes les cellules GEM pour une région donnée, donne une étendue plus large pour R_C et ajoute des informations utiles dans la mesure où les valeurs R_C peuvent également être établies à des emplacements non jaugés. La deuxième approche est probablement un meilleur choix pour des périodes de retour plus longues, compte tenu de la plus grande collecte de données. D'un point de vue pratique, la méthode proposée pour estimer les magnitudes de crue futures est robuste et transférable à d'autres bassins, mais peut bénéficier de l'utilisation de projections de débit provenant d'autres modèles pour une meilleure quantification de l'incertitude.

AKNOWLEDGEMENTS

I would like to express my sincere appreciation to my supervisor, Prof. Laxmi Sushama, for her continuous guidance, encouragement, motivation, and support during my master's degree. I also thank Dr. Muhammad Naveed Khaliq for his help and guidance throughout the course of this work, and Dr. Husham Almansour, Prof. Van-Thanh-Van Nguyen and Prof. Luc Chouinard for their valuable comments.

I would like to thank Compute Canada/Calcul Québec for providing the computational resources.

I extend my gratitude to my lab colleagues for the useful discussions we had, their assistance and their valuable advice and incisive comments that made my work much easier.

I would like to thank my friends for their company, for lending me their ear in difficult times and for all those shared laughs and for being my home in Montreal.

Finally, I would like to thank my family for their endless support. Without their unconditional encouragement, none of this would have been possible.

CONTRIBUTION OF AUTHORS

This thesis has been written following the Graduate and Postdoctoral Studies requirements for a manuscript-based thesis. The main findings of the research undertaken by the author as part of her master's program are presented in a single manuscript. The author carried out the numerical analysis and wrote the manuscript under the supervision of Prof. Laxmi Sushama (supervisor).

The publication detail is presented below:

Maria, D., Sushama, L., Almansour, H., Khaliq, M. N., Nguyen, V.-T.-V., & Chouinard, L. (2024). Future flood envelope curves for the estimation of design flood magnitudes for highway bridges at river crossings. *Results in Engineering*, *22*, 102038.
https://doi.org/https://doi.org/10.1016/j.rineng.2024.102038

TABLE OF CONTENTS

LIST OF FIGURES

LIST OF TABLES

CHAPTER 1 – INTRODUCTION

1.1 Background

Due to the higher water holding capacity of the atmosphere at higher temperatures, an intensification of the hydrological cycle is expected in a future warmer climate, which will likely impact the frequency and severity of extreme hydrological events (IPCC, 2023). Recent incidents underscore the pressing concerns surrounding the vulnerability of transportation infrastructure, notably bridges, to these escalating environmental challenges. This presents a critical challenge to transportation planners, engineers, and policymakers alike to adapt design guidance and maintenance procedures for these changes.

When it comes to structures over rivers, such as dams and bridges, evaluating the maximum flood is a crucial factor, that determines the hydraulic loads it must endure over its operational lifespan. Recent studies on floods, represented in terms of selected return levels of annual maximum daily flows, suggest potential changes in a future warmer climate (Teufel & Sushama, 2021). Therefore, the design and planning of riverine/water infrastructure demand a comprehensive analysis of extreme hydrological events in the context of a changing climate.

The maximum flood used for design purposes could be probable maximum flood, which arises from a combination of extreme conditions such that an event exceeding that is not likely or, in a more conservative approach, could be a specific return level corresponding to the expected useful lifespan of the structure, called the design flood. In Canada, design flood estimation for bridges typically follows guidelines established by authoritative bodies such as the Canadian Highway Bridge Design Code (CHBDC) which suggests a design life of 75 years for new bridge structures, unless otherwise approved by the local regulatory authority in the relevant jurisdiction (Murphy et al., 2018). Statistical frequency analysis is traditionally used in design flood estimation. Since extreme events are rare and historical records are often short, estimation of frequencies of extreme events is challenging. Regional frequency analysis (RFA) (Hosking & Wallis, 1997) is adopted in such situations, which trades space for time by pooling data from several sites in a given homogeneous region.

Engineers frequently employ approaches such as envelope curves to determine the design flood magnitudes. These curves, along with their corresponding equations, are established for specific regions using historical flood data and provide an upper limit for floods within that region. One such commonly utilized envelope curve in Canada is Creager curve. Given climate change, these curves would also need to be adapted to ensure adequate coverage of future situations. Such curves, established for different regions and/or basins, can serve as a quick guidance for obtaining estimated of future design floods.

1.2 Motivation

Bridges play an important role in connecting communities and facilitating the movement of people and goods across rivers which make them critical components of transportation infrastructure. In the Canadian context, where the vast and diverse geography includes numerous rivers and water bodies, the importance of bridges cannot be emphasised enough. However, the changing climate, marked by variations in streamflow/flood magnitudes and patterns, presents a significant challenge to the resilience of these structures.

The climate change induced shifts in streamflow patterns, alterations in precipitation regimes and an increase in the frequency and intensity of extreme weather events over Canada have direct implications for the design and resilience of bridges, as they need to withstand the dynamic forces associated with increasing streamflow, if that is the case. Adapting bridge designs for climate resiliency is imperative to ensure their functionality in the face of evolving hydrological conditions. Recent years have witnessed instances of flood-related damage to bridges across Canada, underscoring the urgency of climate adaptation measures. Notable cases include the catastrophic floods in various regions, such as the floods in Alberta in 2013 and in British Columbia in 2021 that resulted in bridge failures, disruption of critical transportation links, and economic losses. Such events highlight the vulnerability of existing bridge infrastructure.

This study aims to develop an approach, that can be used to apply climate change information into design practices, which can then be used by practitioners without the need for intensive modeling. This is achieved by evaluating correction actors that need to be applied to Creager curves for major river basins in Canada based on estimates of projected changes to extreme events using integrated climate-hydrology model outputs and advanced statistical analysis.

1.3 Research Objectives

The main objective of this study is to develop a framework for adapting flood envelope curves (Creager curve) to a changing climate by estimating correction factors that can be easily used by practitioners by focussing on 7 major river basins in Canada using simulated streamflow based on runoff from a five-member ensemble of Global Environmental Multiscale (GEM) transient climate change simulations. The research aims to achieve the following objectives:

- Conduct an extensive literature review on the probabilistic methods of design flood estimation, the application of climate model outputs to understand the impact on streamflow regimes and flood patterns, on flood envelope curves and their application, and on the effect of climate change on bridge infrastructure.

- Develop a framework for adapting Creager curves to a changing climate through a two phased approach involving construction of Creager curves using observational data for current climate and using transient climate change simulations to develop correction factors for application to current climate Creager curves.
- Apply the developed (2-phased) framework in the Canadian context focusing on major river basins.
- Draw conclusions on the impact of climate change on design flood, represented in terms of correction factors, for different regions in Canada, while identifying/recommending future improvements/studies that can increase the robustness of the results of this study.

1.4 Thesis Outline

This thesis is divided into four chapters: Chapter 1 provides a broad overview of the background, motivation for conducting the study, and objectives. Chapter 2 reviews literature surrounding the effect of climate change on streamflow characteristics, design flood estimation procedures, i.e., regional flood frequency analysis and envelope curves, and the effect of climate change on bridges. Chapter 3 presents the main results of the study presented in the form of a journal article, following the article-based thesis format. Chapter 4 provides additional discussions and lastly, Chapter 5 summarizes the findings, offers ideas for additional pertinent research, and discusses limitations of the study.

CHAPTER 2 – LITERATURE REVIEW

The impact of climate change on transportation infrastructure, including bridges, is a subject of growing concern and pose significant challenges to the resilience and functionality of these systems. Intense precipitation and changes in temperature patterns amongst other anticipated changes to climate variables can contribute to accelerated deterioration, reduced structural integrity, and an increased likelihood of failure of critical infrastructure components. Furthermore, variations in streamflow patterns, influenced by shifts in precipitation and temperature regimes, can lead to heightened flood risks and hydrodynamic loads.

The first part of this chapter discusses the impact of climate change on bridges in Canada and is followed by a section that reviews existing studies on the effect of climate change on precipitation and streamflow characteristics. The review then proceeds to the methods of estimation of design flood magnitudes and development of flood envelope curves. The final part of this chapter reviews some of the existing research on the multifaceted implications of climate change on transportation systems, focusing on bridges.

2.1 Climate change impact on bridges in Canada

Climate change brings about profound impacts on transportation systems, with rising sea levels and intensification of hurricanes, accompanied by stronger winds and higher storm surges, threatening to submerge low-lying infrastructure like coastal highways and ports. Bridges are particularly susceptible to a variety of natural hazards such as flooding, storms, hurricanes, and high winds, and are influenced in multiple ways by shifting climatic conditions. Extremely high temperatures can lead to concrete pavement buckling and asphalt road softening, causing rutting and subsidence. The melting of permafrost in Arctic regions poses significant challenges to road maintenance and design, while the increased frequency of freeze-thaw cycles has the potential to considerably affect pavement designs. Shifting precipitation patterns, with more rain than snow during higher winter temperatures, may exacerbate drainage problems. Precipitation patterns and intensity could change dramatically, affecting the operation of transportation facilities and networks with increased precipitation resulting in increased surface flooding (Meyer & Weigel, 2011; Picketts et al., 2016).

In Canada, recent years have seen a rise in the frequency and severity of flooding incidents, leading to substantial damages and disruptions to bridges across the country. Recent data from Infrastructure Canada reveals a concerning trend in the damages inflicted on bridges by flooding events (Figure 2.1). Between 2010 and 2020, there has been a notable increase in the number of bridge failures or damages attributed to flooding, with an average annual increase of 8%. Moreover, the total cost of repairing or replacing flood-damaged bridges has soared, reaching an estimated $120 million (CAD) annually by 2020, compared to an average of $70 million (CAD) per year in the previous decade. Provinces such as Alberta, British Columbia, and Ontario have experienced particularly severe impacts, with numerous bridges either rendered impassable or requiring extensive repairs following flooding events. For instance, in Alberta, the devastating floods of 2013 resulted in the closure of over 20 bridges and caused damage to countless others, disrupting critical transportation corridors and straining emergency response efforts. Six bridges were destroyed on the Coquihalla during the flooding of 2021, with the total repairs to transportation infrastructures amounting to 1 billion dollars.

Figure 2.1 Flood related damages in Canada. (a-c) Damaged bridges in B.C. from torrential rain that occurred on November 2021; (d) One of two bridges in the Black Diamond/Turner Valley area, Alberta that was washed out during the June flood of 2013; (c) The Highway 83 bridge west of Melita, Manitoba during the flood of July 2014; (f) Morris bridge, in Manitoba, under water during the flood of 2011. (Sources: Global News, The Canadian Press, CBC)

These increasing incidences of bridge failures and damages due to flooding in Canada can be attributed to a combination of factors, including the impacts of climate change as this places a greater strain on bridge infrastructure designed under historical climate conditions. Bridges may be damaged due to local pier scour, channel shift and general scour, ice action on superstructure, exposure of foundations by channel-bed degradation, and overtopping due to hydrodynamic forces that can be attributed to changes in magnitude of peak streamflow.

2.2 Flood processes in Canada and effect of climate change on streamflow

Canada's topographical diversity, coupled with its varied geographical and climatic features, significantly influences precipitation patterns, and streamflow dynamics across the country. The country's topography is characterized by the vast Canadian Shield in the east, the Rocky Mountains in the west, and expansive plains and plateaus in between, which play a crucial role in shaping local climates. This topographical diversity also affects streamflow by influencing drainage patterns, river courses, and the formation of watersheds. This section examines the diverse mechanisms responsible for flooding in Canada, and their projected changes in the context of a changing climate.

In Canada, floods may be generated through snowmelt runoff, flash flooding because of intense rainfall, ice jams or be induced by human activity (Figure 2.2). Snowmelt-driven floods are more frequent in spring and early summer and ice jams are associated with spring breakup of river ice cover, while flash floods generated by intense rainfalls happen in summer when atmospheric convection is more common (Javelle et al., 2002; Clavet-Gaumont et al., 2013; Buttle et al., 2016). For larger basins snowmelt driven by rain-on-snow events characterise the annual maxima, whereas short-duration high intensity precipitation events are often responsible for flood generation in relatively small drainage basins (Watt, 1989).

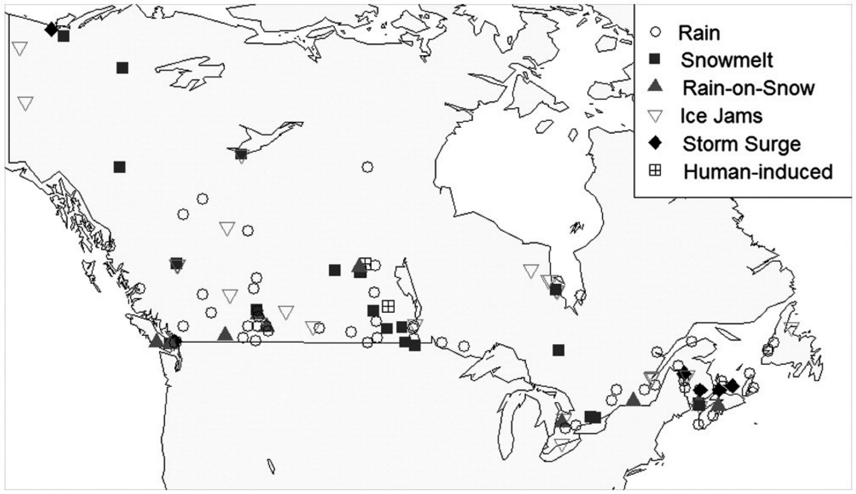

Figure 2.2 Flood disasters in Canada by type between 1990 and 2013 (Buttle et al., 2016).

Progressive warming over the past few decades has resulted in a transition from snowmelt-dominated flooding to rainfall-runoff or rain-on-snow flooding in certain regions. Over recent years several studies have been conducted for different regions within Canada to evaluate projected changes to precipitation and streamflow. They report an intensification of precipitation extremes in future climate (Mladjic et al., 2011; Khaliq et al., 2015; Labonté-Raymond et al., 2020). The evaluation of anticipated changes in streamflow and flooding commonly involves the use of hydrological models driven by climate model outputs for diverse scenarios. There is a growing trend in employing Regional Climate Models (RCMs) to investigate the projected changes in different aspects of the hydrological cycle, including streamflow (Sushama et al., 2006; Poitras et al., 2011; Clavet-Gaumont et al., 2013; Huziy et al., 2013; Jeong et al., 2014; Clavet-Gaumont et al., 2017). Some similar studies using RCMs in Canada, for the eastern, western and the whole region are described below in order.

Huziy et al. (2013) studied 21 Quebec watersheds using streamflow generated by routing runoff from Canadian Regional Climate Model (CRCM) simulations using WATROUTE model. Two different approaches were used in this study for developing projected changes of streamflow characteristics, one based on the concept of ensemble averaging while the other approach was based on merged samples of current and similarly future simulations following multiple comparison tests. They found that the second approach, with longer samples was better at projecting changes to extreme events. Clavet-Gaumont et al. (2013) used RFA approach to estimate return levels for these watersheds and found changes to 5- and 10-year (compared to 30- and 50-year) regional return levels to be statistically significant more often for northern watersheds compared to the rest. The generalized extreme value (GEV) distribution was used to compute return levels of extreme flow events in these studies. Shrestha et al. (2017) undertook non-stationary analysis of extreme streamflow for the Fraser River basin in Canada, using hydrologic model simulations driven by Coupled Model Intercomparison Project Phase 3 (CMIP3) climate simulations and found that the moderate (e.g., 2–20-year return period) extreme streamflow events will decrease in intensity, and little to no change was observed at higher return levels.

Teufel & Sushama (2021) simulated streamflow interactively in GEM using the surface and sub-surface runoff using the modified WATROUTE hydrological routing scheme using an ensemble of five GEM simulations performed for the 1950–2099 period to assess changes to flood-generating mechanisms for both a late 21st century, RCP 8.5 scenario and in a 2° C global warming context in terms of the relative contribution of snowmelt and rainfall, and timing (Figure 2.3). Direct comparison at HYDAT stations where drainage area is within 20% of the value in GEM was used to validate these simulations. They found that in a high warming scenario, the rainfall contribution to streamflow will increase and several regions in southern Canada will become rainfall dominated. These studies also highlight the importance of climate change mitigation, and that expensive flood adaptation measures would be necessary.

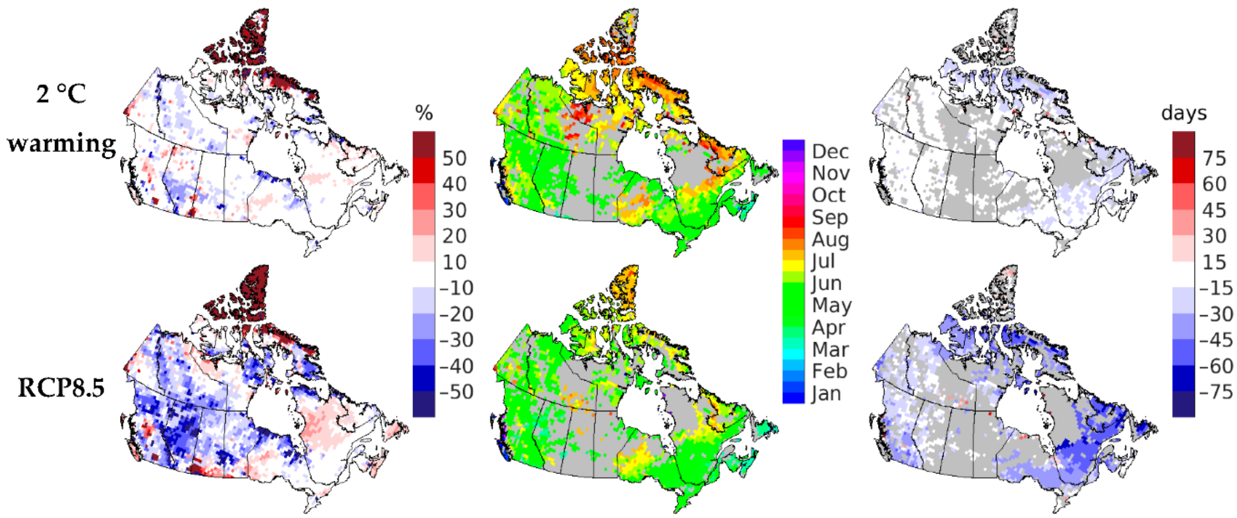

Figure 2.3 Projected changes to median annual maximum streamflow with respect to 1981–2010 (first column), average date of occurrence of annual maximum streamflow (second column), and its projected changes with respect to 1981–2010 (third column). Grey is used for the date at locations where less than 50% of annual maximum events occur within 30 days of the average date (Teufel & Sushama, 2021).

2.3 Estimation of design loads

The design of structures that are to withstand floods, requires computation of either the probable maximum flood (PMF) or the frequency-based design flood. PMF is defined as the maximum flood resulting from the most severe combination of hydrologic and meteorological conditions that are considered reasonably possible for a specific drainage basin (Das et al., 2011). While the PMF itself may never occur, designing infrastructure to withstand such an extreme event helps mitigate risks associated with more common, yet still significant, flood events and this is used for structures that have higher risks associated with them and a larger life span like dams. Bridges crossing rivers are designed to withstand a maximum flood level (design flood) considering the expected frequencies and magnitudes of floods in the area. The design flood level ensures the safety of the bridge without being damaged against historical flooding levels (Habeeb & Bastidas-Arteaga, 2023). Canada's bridge infrastructure is designed based on the CHBDC, which specifies the 75-year flood as the design flood.

The Guide to Bridge Hydraulics describes the hydraulic considerations for bridge planning, design and construction, and the analysis and estimation of streamflow and associated water levels for bridge design and evaluation for Canada. Methods used to estimate design floods can be divided into three main categories: (1) statistical frequency analysis of streamflow data; (2) runoff modelling using data or statistics on rainfall and/or snowmelt as input; and (3) empirical methods such as the Rational Method, flood peak/drainage area relations. In some regions and jurisdictions, the magnitude of a design flood or storm for a particular site may be specified based on a previously experienced historical event called regulatory flood or storm. Runoff modelling represents a quite different approach from statistical frequency analysis of streamflow data, where selected precipitation sequences, and snow/temperature sequences where appropriate, are used as inputs to a numerical model which predicts the runoff and streamflow, which is then used to estimate design flood. Rainfall based methods are used when no, or inadequate, streamflow data are available at the site of interest.

Frequency analyses for bridge design purposes are normally based on series of annual maximum discharges. The analysis may be performed at a single site, or preferably a regional approach can be adopted when estimating floods corresponding to longer return periods. Regional approaches can also be used to estimate events where no information exists (ungauged) at a site (Pilon &

Adamowski, 1992). A summary of common approaches to design flood estimation is given in Figure 2.4.

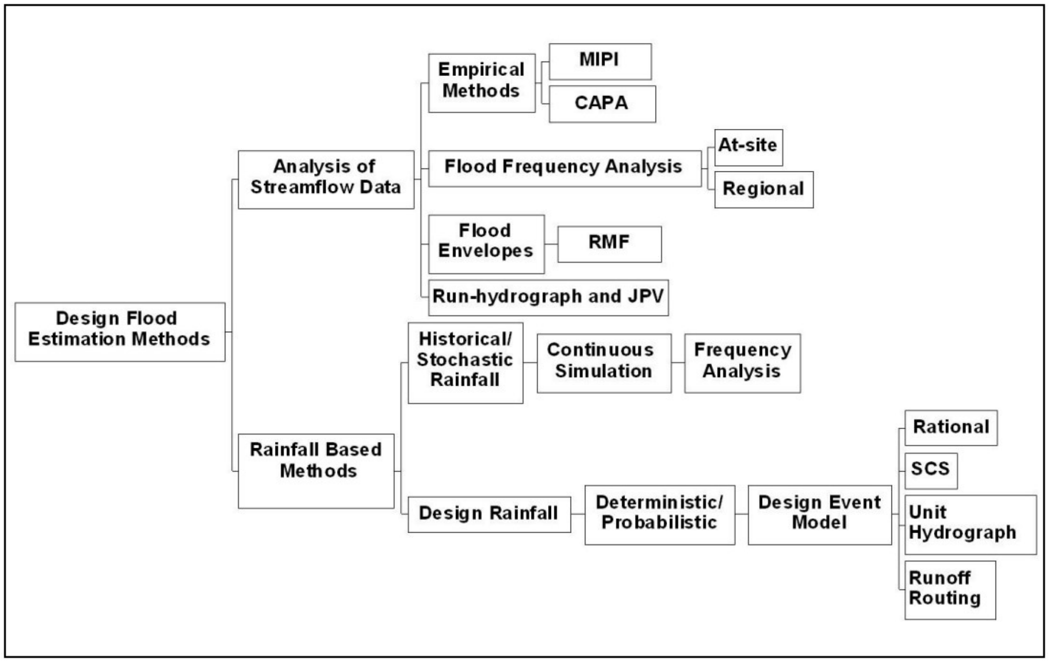

Figure 2.4 Design flood estimation methods (Smithers & Schulze, 2001). The Catchment Parameter method (CAPA), Pitman and Midgley method (MIPI) are commonly used empirical methods in South Africa. Regional maximum flood (RMF), Joint peak volume (JPV) and Soil Conservation Service (SCS) methods are also used to derive flood estimates.

Even though design flood estimation and flood-management are usually done as small scale studies, some broad scale studies can also be found in the literature. Smith et al. (2015) carried out regional flood frequency analysis (FFA) at the global scale using annual maximum flows from 703 gauges from the Global Runoff Data Centre. Faulkner et al. (2016) derived preliminary design flood flows for 24,000 locations throughout Canada on rivers with catchments larger than 400 km^2 using FFA of instantaneous and daily annual maximum flows at 1664 gauging stations that was regionalized using geostatistical methods (Figure 2.5).

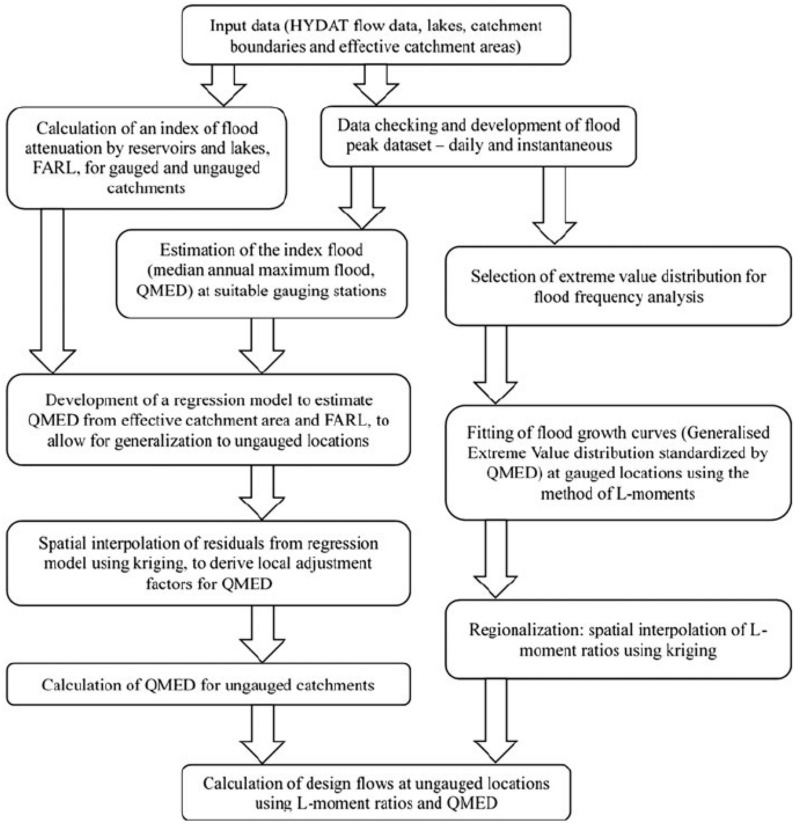

Figure 2.5 Flow chart of method for estimating design floods for all of Canada (Faulkner et al., 2016)

2.2.1 Regional frequency analysis

The framework proposed in this study uses regional frequency analysis (RFA) of streamflow data to derive the design flood of interest. This section reviews some of the key steps of RFA. Two main methodologies in use today for RFA are: regional quantile regression approach and the index-flood approach which describes a regional quantile growth curve estimated graphically or by statistical methods. The index flood procedure (Dalrymple, 1960) is the basis for the L-moments based RFA approach that was formalised by Hosking & Wallis (1997). This section focuses on RFA utilizing the L-moments-based index-flood approach, and the process involves the following steps: (1) Screening of data, (2) Defining homogeneous regions, (3) Choosing a frequency distribution for each region and assessing its robustness, (4) Estimate flow quantiles for both gauged and ungauged sites.

Statistical tests become necessary to screen out outliers and then to check whether they can be accepted within a homogeneous group. There are many tests for outliers. In the context of RFA using L-moments, Hosking & Wallis (1997) found that comparing sample L-moment ratios of different sites using a measure of discordancy between the L-moment ratios of a site and the average L-moment ratios of a group of similar sites, called the discordancy measure (D_i), provides useful information. The following equations are used to calculate the first four sample L-moments in terms of probability weighted moments (b_r) for a site with n observations:

$$l_1 = b_0 \tag{1}$$

$$l_2 = 2b_1 - b_0 \tag{2}$$

$$l_3 = 6b_2 - 6b_1 + b_0 \tag{3}$$

$$l_4 = 20b_3 - 30b_2 + 12b_1 - b_0 \tag{4}$$

The probability weighted moment b_r of order r is given by:

$$b_r = n^{-1} \sum_{j=r+1}^{n} \frac{(j-1)(j-2)\ldots(j-r)}{(n-1)(n-2)\ldots(n-r)} x_{j:n} \tag{5}$$

where $x_{j:n}$ are the ordered sample values. L-moment ratios are dimensionless versions of L-moments and are defined as:

$$t_2 = l_2/l_1 \text{ (L-CV)} \tag{6}$$

$$t_3 = l_3/l_2 \text{ (L-skewness)} \tag{7}$$

$$t_4 = l_4/l_2 \text{ (L-kurtosis).} \tag{8}$$

The regional average L-moment ratios for a region R with N sites, with respective sample sizes n_1, n_2,.., n_N are then given by:

$$t_r^R = \frac{\sum_{i=1}^{N} n_i t_r}{\sum_{i=1}^{N} n_i}, r = 2, 3, 4. \tag{9}$$

If $\boldsymbol{u}_i = [t_2^{(i)}, t_3^{(i)}, t_4^{(i)}]$ be the vector containing the L-moment ratios of site i and $\overline{\boldsymbol{u}}$ is the vector of unweighted regional average L-moment ratios, the discordance measure for site i is defined as:

$$D_i = \frac{1}{3}(\boldsymbol{u}_i - \overline{\boldsymbol{u}})^T \boldsymbol{A}^{-1}(\boldsymbol{u}_i - \overline{\boldsymbol{u}}), \tag{10}$$

where $\boldsymbol{A}$ is the sample covariance matrix, defined as:

$$\boldsymbol{A} = (N-1)^{-1} \sum_{i=1}^{N} (\boldsymbol{u}_i - \overline{\boldsymbol{u}})(\boldsymbol{u}_i - \overline{\boldsymbol{u}})^T \tag{11}$$

and T denotes transpose of a vector or matrix.

The sites having D_i values higher than the critical value (Table 2.1) are either removed from the set of data or moved to a different region.

Table 2.1 Critical values for discordancy measure *(D_i)* (Hosking & Wallis, 1997)

Number of Sites	7	8	9	10	11	12	13	14	≥15
Critical Value	1.917	2.140	2.329	2.491	2.632	2.757	2.869	2.971	3

Identifying homogeneous regions stands out as the most challenging part of RFA and demands subjective evaluation. The primary objective is to create clusters of sites wherein their frequency distributions match closely, differing only in terms of a site-specific scale factor (Hosking & Wallis, 1997). Sites may be organized for convenience based on geographical proximity, especially in studies focused on administrative regions. However, this grouping method does not assure homogeneity, as neighboring basins might exhibit physical differences (Acreman & Sinclair, 1986).

For small scale studies regions can be defined subjectively by inspection of the site-characteristics, which is then tested for heterogeneity. Gingras et al. (1994) used the time of year when the largest flood occurred as the parameter to delineate sub regions in Ontario and Quebec and Decoursey (1972) created groups of basins in Oklahoma based on their analogous flood responses. Sites can be divided into groups depending on whether their site characteristics exceed one or more threshold values, referred to as objective partitioning, where threshold value is chosen to minimize a within-group heterogeneity criterion. Mailhot et al. (2013) used the peaks-over-threshold approach to for regional frequency analysis of rainfall extremes in southern Quebec.

Cluster analysis is a standard method of statistical multivariate analysis that has been successfully used for dividing data into homogeneous groups for RFA (Tasker, 1982; Clavet-Gaumont et al., 2013; Faulkner et al., 2016). A data vector represents the characteristics of a site, and the sites are grouped according to the similarity in their respective characteristics. Other alternative methods of defining homogeneous regions include the method of residuals, canonical correlation analysis, and region-of-influence (ROI) (Burn, 1990; Gado & Nguyen, 2016; Mostofi Zadeh & Burn, 2019; Zhang & Stadnyk, 2020).

Once the regions or sub-regions are identified, their homogeneity is evaluated using formal statistical testing to ensure application of regional flood frequency analysis framework. It determines whether the region should be divided into smaller regions or if two or more regions can be combined into one. Statistical homogeneity can be assessed through various methods, including the Dalrymple test (Dalrymple, 1960), CV-test (Lettenmaier et al., 1987), S-test (Pilon et al., 1991), R-test (Wiltshire, 1986), and the most commonly used H-test (Hosking & Wallis, 1997). The method involves comparing the variability of L-moment ratios among sites within a region with the expected variability derived from simulations using a set of sites with a record length equivalent to the corresponding observations. A measure of heterogeneity is subsequently computed by assessing the disparity between the weighted standard deviation of L-CVs (coefficient of variation of L-moments) across sites in the region and the corresponding mean statistics obtained from simulations. Supposing that the selected region has N sites, with the ith site having a record length of n_i and t_r^R as defined above, the following V and H statistics are calculated for the region,

$$V_k = \left[\sum_{i=1}^{N} \frac{n_i\left(t_r^{(i)} - t_r^R\right)^2}{\sum_{i=1}^{N} n_i}\right]^{\frac{1}{2}}, r = 2, 3, 4; k = 1, 2, 3 \tag{12}$$

$$H_k = (V_k - \mu_{V_k})/\sigma_{v_k} \tag{13}$$

The statistics V_1, V_2 and V_3 respectively correspond to L-CV, L-skewness and L-kurtosis. μ_{V_k} and σ_{V_k} are the expected mean and standard deviation of a homogenous group, and H_k is a measure of the variability of L-moment ratios in the region compared with that expected for simulated homogeneous regions. Hosking & Wallis (1997) suggested a 4-parameter Kappa distribution for generating simulated homogenous regions.

After confirming the homogeneity of a region, a single frequency distribution is fitted to the pooled data from all sites within the region. Some reasonably flexible candidate distributions are usually evaluated for the accuracy of the quantile estimates for each site. Different distribution functions have been evaluated in previous studies over Canada (Yue & Wang, 2004; Aucoin et al., 2011; Clavet-Gaumont et al., 2013; Huziy et al., 2013; Yang, 2016), which generally demonstrate that the GEV distribution fits Canadian annual maximum flow data considerably better than other well-known distributions, including generalized logistic, Pearson Type III, and log Pearson Type III distributions.

Once a target region is found to be homogeneous and a probability distribution function is determined, it is assumed that the probability distribution of all sites in the region is identical except for the site-special scaling factor known as the index flood which is usually the mean annual flood or the median annual flood. Various flow quantiles at any given site within the region can be estimated as the product of the index flood and the growth factors obtained from the regional growth curve or the regional frequency distribution function corresponding to selected return periods or exceedance probabilities of interest.

2.2.2 Envelope Curves

As mentioned earlier, flood envelope curves are a commonly used tool for design flood estimation in Canada and in other parts of the world. The main objective of this study is to adapt these curves to climate change. This section provides information on several commonly employed envelope curves. For a given region containing several river basins, these curves determine the upper limit of floods when maximum values of the floods are plotted against respective drainage areas, and they are often associated with nonlinear functional relationships. In general, the largest observed floods are plotted against drainage area, both on logarithmic axes, and an envelope is drawn enclosing all data points. These curves can be global or regional and can also be developed using floods corresponding to selected return periods of interest (Chaves et al., 2017).

The very first envelope curve was established by Jarvis (1926), who formulated the maximum flood envelope curve for the United States from the analysis of 888 fluviometric stations. This was later improved upon by Crippen & Bue (1977) and Crippen (1982) by creating another 17 curves and analyzing a total of 883 stations. Creager et al. (1945) formulated another mathematical equation for the calculation of the envelope curves based on data from 760 stations, including 730 from the United States and the remaining from other countries (Figure 2.6). This equation, known as Creager curve, has been widely used in many parts of the world. Francou & Rodier (1967) also developed mathematical formulation of the envelope curve, which is widely used in several countries. Castellarin et al. (2005) proposed a new methodology for the development of these curves, which was later improved in Castellarin (2007). The most used envelope curves are Creager, Francou-Rodier, Castellarin, Matthai and Crippen.

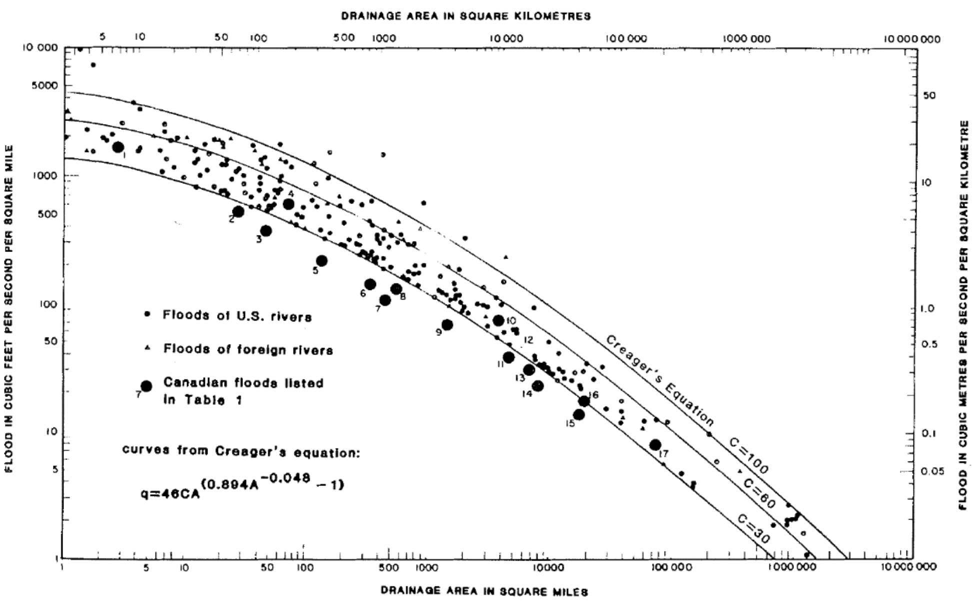

Figure 2.6 Unusual flood peaks from Canada superimposed on Creager's original plot (Creager et al., 1945)

The Creagers curve is given as :

$$q = 46CA^{0.894A^{-0.048}}, \tag{14}$$

where q is the specific peak flow in ft³/sec per unit drainage area and A is the drainage area in square miles.

The envelope curve of Francou&Rodier (1967) is commonly used in Europe and Africa and can be expressed as:

$$\frac{Q}{Q_0} = \left(\frac{A}{A_0}\right)^{1-\frac{k}{10}}, \tag{15}$$

where Q is the maximum flow rate in m^3/s, Q_0 = 106 m^3/s, A the drainage area in km^2, A_0 = 108 km^2 and k the Francou-Rodier's regional coefficient, is given by:

$$k = 10\left[1 - \frac{\log Q - 6}{\log A - 8}\right]. \tag{16}$$

The curve proposed by Castellarin et al. (2005) is represented as:

$$\ln\left(\frac{Q_{\max}}{A}\right) = a + b\ln(A), \tag{17}$$

where Q_{max} is the maximum flow rate for a given fluviometric station (in m^3/s), a and b are regional constants of the regression and A is the drainage area.

Matthai (1969) used only a basic envelope equation, which relates the drainage areas to the maximum flow rate as:

$$q = \alpha A^{\beta}, \tag{18}$$

where q is the maximum flow rate, A is the drainage area and α and β are regional parameters.

The methodology proposed by Crippen (1982) is based on the curve given by:

$$q = k_1 A^{[k_2 - 1]}(A^{0.5} + 5)^{k_3}, \tag{19}$$

where q is the maximum flow rate, A the drainage area and k_1, k_2, and k_3 are the regional coefficients empirically determined.

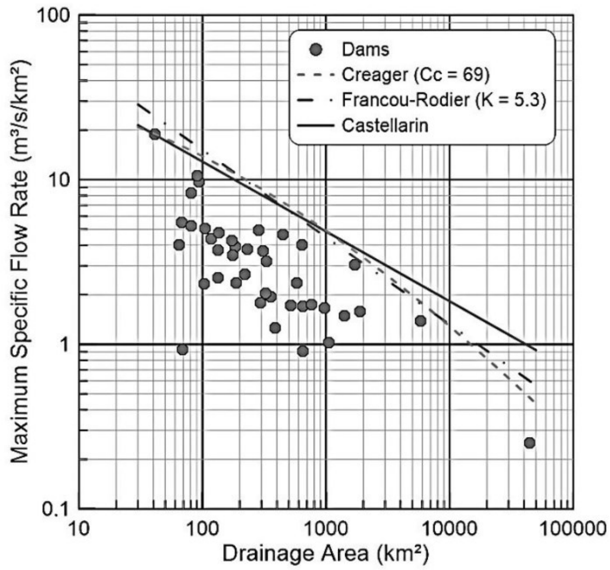

Figure 2.7 Creager's, Francou-Rodier's and Castellarin's curves comparative analysis for 1,000-year return period flow rate in Ceará (Chaves et al., 2017).

Chaves et al. (2017) applied three envelope curves (Creager's, Francou-Rodier's and Castellarin's curves**)** to watersheds in Ceará, Brazil. Based on the estimation of new regional parameters for Ceará, they constructed envelope curves for floods of 1,000 (Figure 2.7) and 10,000-year return periods using extended historical flood data which were used for investigating safety of existing hydraulic structures. Ahsan et al. (2016) conducted a similar study in Pakistan for Indus and Jhelum River basins, and developed Creager curves for each basin using FFA of maximum observed flows.

Lima et al. (2017) assessed peak streamflow observed in many regions in Brazil to estimate the 10,000-year return levels and compared them to the Creager envelope curves. They found that Creager's coefficient (*C)* between 60-100 can define all floods. However, for regions with smaller drainage areas, this range overestimates the design flood and hence they recommended using different values of *C* (Figure 2.8).

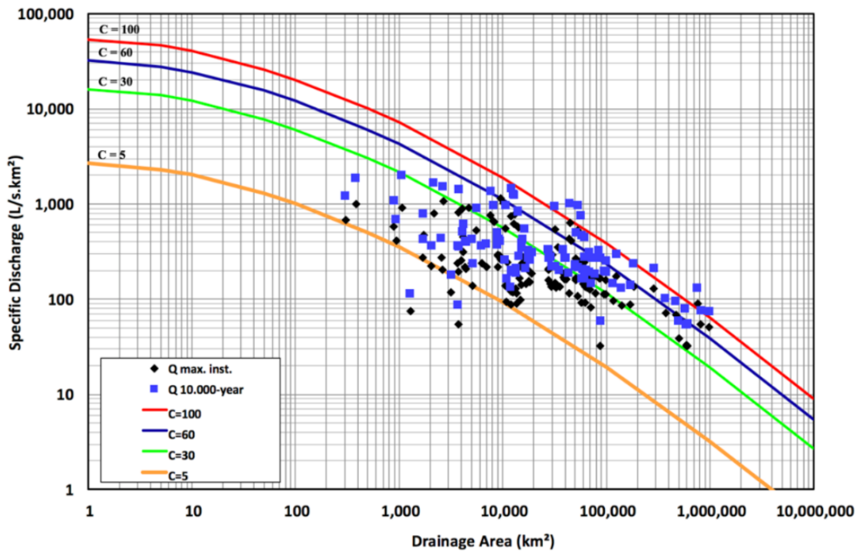

Figure 2.8 Specific observed instantaneous floods and 10,000-year return period floods and Creager envelope curves for Brazil (Lima et al., 2017)

2.2.3 Flood envelope curves for Canada

In Canada, flood management is often done at the provincial level and a few studies have been conducted in certain regions of Canada where envelope curves were used as design flood evaluation tools which are discussed in this section.

In Ontario, FFA was undertaken for the Great Lakes watershed system to estimate the flood magnitudes corresponding to different return periods, using annual maximum peak instantaneous streamflow (MNRF, 2014). They superimposed the Creager envelope curve on the maximum floods, which were found to fit well the Creager coefficient of 10. The lower value of the coefficient indicate that floods in the Great Lakes watershed are relatively low when compared to other regions.

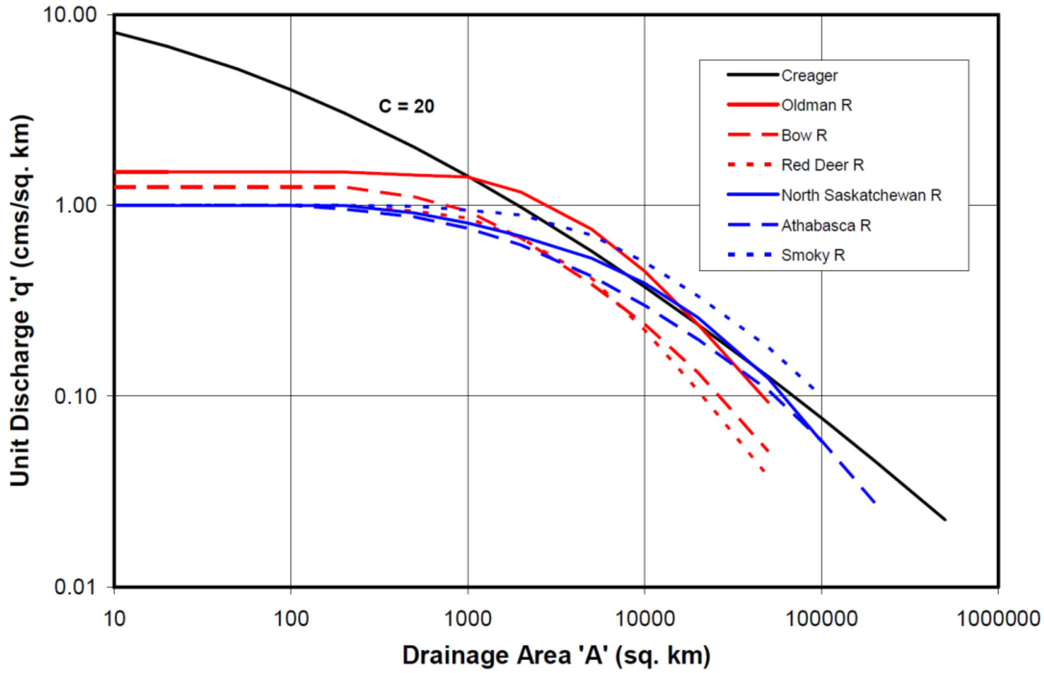

Figure 2.9 Visual fitted envelope curves for different river basins from Alberta superimposed with Creager curve (C=20) (Alberta Transportation , 2007)

In Alberta, Creager curves were developed for six basins using instantaneous peak flow data. Plots of q vs. A on a log-log plot were prepared for each of the major river basins and points that stood out from these plots were evaluated to assess the confidence in the data (Alberta Transportation, 2007). They added Creager envelope curves to each of the plots along with additional envelope curves based on both a simplified model and a visual fit (Figure 2.9). Additional curves were employed to assess the variations between basins in terms of curve fitting accuracy.

In New Brunswick, FFA was carried out to determine the characteristics of high flow events (Aucoin et al., 2011). They conducted single stations analyses for 56 hydrometric stations located mainly in the New Brunswick watersheds, with one station from Nova Scotia. A regional flood frequency analysis was also carried out in this study using both quantile regression and the index flood approach. Envelope curves were constructed using instantaneous peak flows and the maximum ratio of the instantaneous peak flow to mean flow (QP/QD) was also considered, and its relationship with the drainage area was also studied, which they applied to mean flow to derive instantaneous peak flow values. This was then compared with envelope curves from previous studies (Figure 2.10) and they found that addition of more data points added value.

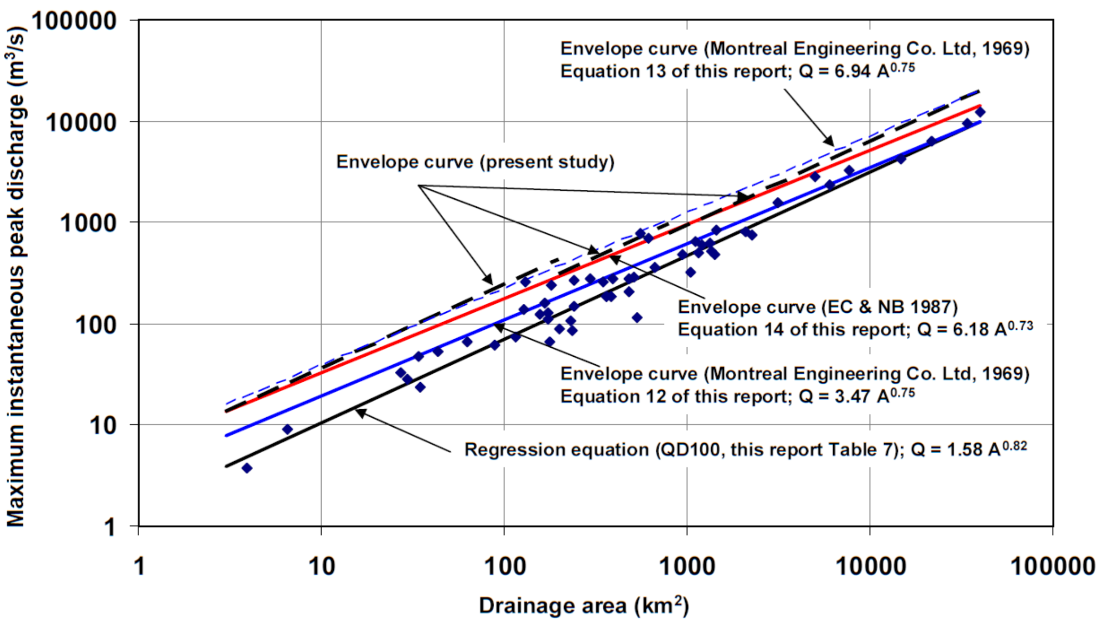

Figure 2.10 Envelope curves of the study region, developed based on instantaneous peak flows (m3/s) in relation to those of previous studies. Data points represent the maximum instantaneous flow (highest recorded flow) for each station in NB (Aucoin et al., 2011).

A protocol to estimate probable maximum flood (PMF), peak flows and runoff volumes based on past studies of PMFs was developed for British Columbia (Abrahamson, 2010). This study assembled the results from the detailed PMF studies for these projects and correlated the flood peaks and volumes to the drainage area to develop equations, and envelope curves that can be used to estimate the PMF potential at other sites. They found that the shape of the Creager curve showed a good relationship with the British Columbia data.

2.4 Effect of climate change on Bridges

One of the key effects of climate change on bridges will be the increased risk of scour of bridge piers and abutments (Dawson et al., 2016). Several studies have been conducted that evaluated risks associated with climate change on bridges, a few of which are discussed in this section along with some studies that focus on adaptation strategies.

Devendiran et al. (2021) evaluated the multi-hazard impact considering climate change in terms of risk and resilience of the existing bridge spanning over the San Joaquin River, California using future flood projections under climate change obtained from general circulation model simulations in conjunction with a macroscale hydrological model. A similar study was conducted by Habeeb & Bastidas-Arteaga (2023) for a railway bridge in United Kingdom using river flow values from a hydrological model driven by a regional climate model providing insights into vulnerability assessment of bridge structures due to potential increases in riverine flooding. Bhatkoti et al. (2016) evaluated the consequences of climate change on bridge design flood by considering return frequency for precipitation from both the current and future climate intensity-duration frequency (IDF) curves generated from observations and climate models respectively. IDF curves for current and future climates were directly compared in this study to quantify the effects of climate change as increases in probability of the events. These studies have found that enhanced intensities of future design floods cause higher expected scour at around bridge piers resulting in significant rise in risk and drop in resilience, compared to no climate change scenario.

Design procedures are currently developed around the statistical analysis of past events. The design flood loads, and exposure categories are assumed to be the same in the future. A reassessment of design loads and exposure categories for sea-level rise, hurricanes, temperature and precipitation is essential to the adaptation process (Mondoro et al., 2018) and incorporating climate change into bridge design considerations have been recommended by numerous studies (Murphy et al., 2018; François et al., 2019; Khaliq, 2019; Othman et al., 2019; Coulbourne et al., 2021; Kundzewicz & Licznar, 2021). Many researchers have also developed systematic frameworks and tools for assessing vulnerability to climate change and have proposed updating existing guidelines and standards updates to reflect evolving climate risks, ultimately aiming to enhance infrastructure resilience. Darch & Jones (2012) used climate model outputs to directly alter parameters in the UK Flood Estimation Handbook rainfall–runoff model to adapt design flows for changes in climate for the Eden catchment in northwestern England by defining change factors that were applied to historical data. Kumar (2023) proposed a framework for design flood estimation in India by calculating the design flood using an L-moment based approach and studying the effect of climate change using the CMIP-5 scenarios and applying fixed percentage increases. du Plessis&Masule (2023) developed revised flood envelope curves for South Africa that were drawn 15% above the observed maximum flows to account for climate change. Othman et al. (2019) investigated the applicability of the current design climate loads of the Canadian Highway Bridge Design Code (CHBDC) to model current and future climatic actions. They studied climate loads including daily temperatures (maximum, and minimum), relative humidity, and hourly mean wind pressures (for 50- and 100-year return periods) using the climatic design loads of CHBDC, that were then compared with the current loads estimated based on homogenized climatic data from Environment and Climate Change Canada’s national archives. Wasko et al. (2021) conducted a review of different methods for integrating climate change information into Flood Frequency Analysis (FFA) and discussed the pros and cons of scenario-driven and scenario-neutral approaches, and the uncertainties inherent in FFA. They also emphasized the absence of a consensus methodology for estimating design floods in a changing climate.

2.5 Knowledge gaps and conclusion

River crossing bridges are essential elements of the transportation network, and they play a pivotal role in ensuring the seamless flow of goods, services, and people across regions. The resilience and adaptation of river crossing bridges are important, especially in the face of climate change-induced intensification of future flooding. Numerous studies have investigated the regional variations in climate change effects on bridges and associated risks and challenges. Proper understanding of the specific impacts on these structures, particularly from floods, is crucial for ensuring their longevity, safety, and continued functionality. This understanding is imperative in the context of adapting existing bridges to the potential impacts of climate change and for designing new ones by integrating climate change considerations in the design methodology.

Despite considerable research surrounding climate change modelling and impact analysis for different parts of Canada, studies on bridge-climate-flooding interactions have been lacking, especially those related to adaptation of design flood estimation procedures for river crossing bridges. There is a critical gap between the availability of relevant guidance and its practical implementation for climate change adaptation of bridge design practices. By focusing on the practical integration of climate change projections with design flood estimation procedures, this research endeavors to develop applicable guidance for engineering practitioners, by developing a framework for developing climate change informed flood envelope curves, which can be used for designing of new structures and evaluating flood-resilience of existing ones.

This thesis addresses some of these knowledge gaps and contributes towards the development of a framework for adapting Creager's flood envelope curves to climate change through correction factors, estimated using streamflow projections based on the Global Environmental Multiscale (GEM) model.

CHAPTER 3 - FUTURE FLOOD ENVELOPE CURVES FOR THE ESTIMATION OF DESIGN FLOOD MAGNITUDES FOR HIGHWAY BRIDGES AT RIVER CROSSINGS

Dona Maria[1*], Laxmi Sushama[1], Husham Almansour[2], Muhammad Naveed Khaliq[3], Van-Thanh-Van Nguyen[1], Luc Chouinard[1]

[1]Department of Civil Engineering, Trottier Institute for Sustainability in Engineering and Design, McGill University, Montreal, QC, Canada

[2]Construction Research Centre, National Research Council Canada, Ottawa, ON, Canada

[3]Ocean Coastal and River Engineering Research Center, National Research Council Canada, Ottawa, ON, Canada

*Corresponding author

Email: dona.maria@mail.mcgill.ca

Abstract

Creager flood envelope curves, which serve as the upper bound/limit of observed extreme flows, are commonly used by practitioners to estimate design flood magnitudes, which in the case of most river-crossing highway bridges is 75-year flood magnitude in Canada. This study proposes a novel framework for climate change adaption of Creager curves for estimating future design floods. These curves, for the current period, are assessed considering 417 observation stations, located in seven major Canadian river basins (i.e., Fraser, Nelson, Mackenzie, Yukon, Churchill, St Lawrence and St John). The Creager coefficient C, which defines flood envelope curves, varies between 1-45 across the studied river basins. To adapt Creager curves for future changes in streamflow, a correction factor, R_C, which is the ratio of future to current period C values, is proposed. These factors are obtained for observation sites, using streamflow data from an ensemble of Regional Climate Model (RCM) simulations for current and future periods, through two Regional Frequency Analysis approaches. The first approach, considering only the RCM cells where the stations are located, suggests R_C in the 0.3-1.6 range, with southeasterly basins showing values < 1. The second approach, considering all RCM cells for a given region, yields a wider range for R_C and adds useful information in that R_C values can also be established at ungauged locations. From a practical viewpoint, the proposed framework for estimating future design floods is robust and transferrable to other basins, but can benefit using streamflow projections from other models for better uncertainty quantification.

Keywords: Climate change; Creager curves; Design floods; Bridges; Regional flood frequency analysis; Regional climate modeling

3.1 Introduction

Floods are one of the most frequent and costliest of natural disasters resulting in considerable economic losses and social repercussions. Due to considerable variations in regional climate, landforms and topographical features, flood characteristics (intensity, frequency and time of occurrence) and flood generating mechanisms vary across Canada. They are primarily driven by spring snowmelt, rain-on-snow events, ice jams, single- and multi-day heavy rainfall events or a combination of these (Watt, 1989). Furthermore, an increase in the frequency and intensity of extreme events, including floods, is anticipated in a future warmer climate, which can further exacerbate flood-related impacts (Bush & Lemmen, 2019; Teufel & Sushama, 2021). Previous climate change impact assessment related studies over Canada have projected changes in future flood patterns, magnitudes and seasonality over Canada (Poitras et al., 2011; Clavet‐Gaumont et al., 2013; Huziy et al., 2013; Jeong et al., 2014; Clavet-Gaumont et al., 2017; Teufel & Sushama, 2021). The findings of Bonsal et al. (2019), who documented projected changes in Canadian streamflow for the mid-to-late 21st century, and those of St‐Jacques et al. (2018) and the above-mentioned studies suggest that not all river basins will respond in the same way to climate change in the future. Under low and medium emission scenarios, the spring peak flow for southern rivers in the middle of the 21st century is expected to occur earlier and will be smaller in magnitude (Bonsal et al., 2019).

Understanding future flood characteristics plays a key role in many engineering applications, especially in the design of dams, culverts, bridges, embankments and similar other structures (Aucoin et al., 2011). Selection of an appropriate design flood magnitude is critical in the design of these structures. This can be the probable maximum flood (PMF) for high-capacity structures (e.g., large dams and floodwalls). The PMF results from the most severe combination of meteorological and hydrologic conditions that can reasonably be expected over a basin. In the estimation of PMF, the critical meteorological condition that is generally considered is a reasonable estimate of probable maximum precipitation, while its hydrologic counterpart is either assessed with a high wetness index for summer-fall conditions or a large snowpack for winter conditions (Beauchamp et al., 2013). The PMF is usually several times greater than the flood of record available through instrumental records (Smith, 1993). A more conservative design flood is an estimate that corresponds to a selected return period such that an event exceeding that will not likely occur during the useful lifetime of the structure. The return period considered depends upon the intended lifetime of the structure and is generally longer for critical structures, which could cause severe damage and loss of life in case of failure. These design values are usually calculated through flood frequency analysis (FFA), employing high flow sequences derived from observational streamflow records or rainfall-runoff model simulated flow sequences, or using empirical equations that relate frequency-based flood magnitudes (e.g., 100-year flood) with basin attributes (e.g., drainage area, mean annual precipitation, mean annual temperature, drainage density, mean basin slope, mean basin elevation, land cover, etc.). The latter approach, which is well established in ungauged hydrology, is applicable where observational records are not available or where the available limited records cannot support a reliable FFA.

In the design context, flood envelope curves are often used for preliminary evaluation of design floods for sizing various structures and for checking the design basis of old structures to verify their safety and compliance with updated standards and guidelines. These curves, associated with a mathematical equation linking extreme floods or PMF with drainage area or accumulation area, provide upper limits for floods in a basin. Different envelope curves have been proposed in the literature of which the commonly used are Creager, Francou-Rodier, Castellarin, Lowry, Matthai and Crippen (Francou & Rodier, 1967; Crippen, 1982; Castellarin et al., 2005; Chaves et al., 2017), with some studies focussing on developing regional envelope curves tailored to specific regions. Applications of these can be found in Chaves et al. (2017), Abdullah et al. (2019), Ahsan et al. (2016), Ewea et al. (2020), Saharia et al. (2017), Bertola et al. (2023), and Lima et al. (2017). It is important to mention that regression relationships relating peak discharges or design flood discharges with catchment attributes should not be confused with envelope curves. While these regression relationships represent an average behavior, an envelope curve encompasses all floods and acts as an upper bound, which is the definition followed in this paper.

The Creager curves were first published in 1945, based largely on U.S. flood data (Creager et al., 1945). These curves were later updated to include selected major floods from Canada (Neill, 1986; Watt, 1989). As these curves were developed based on the past flood events available at the time, some studies have shown that inclusion of additional data, especially recent peak flood events, can shift these curves upwards (Abrahamson, 2010; Aucoin et al., 2011). It is believed that one single Creager curve for Canada is insufficient as some studies have shown that eastern regions and prairies, when compared to the western regions of Canada, have different values of the controlling parameter (Alberta Transportation, 2007; Abrahamson, 2010; MNRF, 2014), with the latter regions having higher magnitude of floods. Creager curves are typically developed using instantaneous peak flows, but they can also be developed using PMFs, maximum mean daily flows, selected flood return levels of interest or other indices of interest, reflective of extreme flood characteristics.

Estimation of design flood magnitudes and associated loads for infrastructure design purposes should factor in climate change (Murphy et al., 2018; François et al., 2019; Khaliq, 2019; Othman et al., 2019; Coulbourne et al., 2021; Kundzewicz & Licznar, 2021). In the context of Creager curves, this entails adaptation of these curves, either by integrating correction factors with the underlying methodology or by developing new curves based on alternative approaches. In some studies, site-specific changes to design flood magnitudes have been developed. For example, Quintero et al. (2018) developed changes to the 100-year flood for the Cedar and Skunk River basins in the United States by integrating downscaled rainfall projections with a hydrological model for producing flow sequences and thereby conducting FFA. Similarly, Awasthi et al. (2022) used precipitation and temperature projections from Global Climate Models (GCMs) within a generalized regression model setting to develop changes to design flood magnitudes by generating sequences of annual maximum flood flows and performing FFA. In South Korea, Kwon et al. (2011) developed design flood magnitudes using a precipitation-runoff model for different climate change scenarios. In India, Tofiq & Güven (2015) projected daily inflows to Darbandikhan dam using outputs from GCMs and developed projected changes to design flood values by conducting FFA of both observed and simulated inflows. du Plessis & Masule (2023) developed revised flood envelope curves for South Africa that were drawn 15% above the observed maximum flows to account for climate change. Using a climate-hydrology coupled integrated regional climate modeling approach, Sushama et al. (2006), Huziy et al. (2013) , Clavet-Gaumont et al. (2017) and Jeong et al. (2014) have developed projected changes to various flood characteristics for select Canadian river basins. Recently, Wasko et al. (2021) reviewed various approaches for incorporating climate change information in FFA. While discussing the advantages/disadvantages of climate change scenario-driven and scenario-neutral approaches, and uncertainties encountered in FFA they also highlighted that no consensus methodology exists for estimating design floods in a changing climate. In many of the references cited above, investigators have also discussed various possibilities for integrating climate change information with FFA methods and estimating uncertainties based on ensemble modeling techniques i.e., considering multiple models, multiple scenarios, and multiple future time horizons, along with consideration of expected lifespan of design projects. In addition to this, Ahmadi & Ahmadi and Habeeb & Bastidas-Arteaga (2023) respectively provide guidance on bridge codes and vulnerability assessment of bridge structures due to potential increases in riverine flooding.

A Canada wide study is currently lacking that considers the application of Creager curves by considering the effects of climate change on design floods for various engineering design purposes. Thus, this study aims to fill this gap by developing a framework for generating climate change informed Creager curves that can easily be adopted by practitioners for design purposes and conducting flood-vulnerability assessments by focussing on seven large river basins spread across Canada that cover many important economic and commercial hubs as well as regions containing vast network of river crossing highway bridges. Additionally, the study aims to simplify the process of climate change adaptation of design floods for planners and project engineers by eliminating the need for resource-intensive and time-consuming modeling endeavors. Climate change adaptation of Creager curves has not been attempted before, which is the novel contribution of this study.

This paper is structured as follows. Description of the methodology adopted for integrating climate change information with Creager curves is provided in Section 2, along with the description of observational dataset and regional climate model (RCM) simulations employed in the study. Results of the study and associated discussions and insights are provided in Section 3. Main conclusions of the study, usefulness of the developed framework, and future research directions are presented in Section 4.

3.2 Study area, data and methods

The proposed framework for adapting Creager flood envelope curves (Creager et al., 1945) in a changing climate consists of two main parts. The first part deals with establishing Creager curves in current climate considering observation stations in the study area, which encompasses seven major Canadian river basins: Fraser, Nelson, Mackenzie, Yukon, Churchill, St Lawrence, and St John (Figure 3.1.b). The Creager flood envelope curve, originally developed in the FPS system, is given by (Creager et al., 1945):

$$q = 46CA^{0.894A^{-0.048}} \quad , \tag{1}$$

where q is the specific peak flow in ft^3/sec per unit drainage area and A is the drainage area in square miles. In the present study, MKS system of units is used by incorporating respective conversion factors in Eq. (1) and considering flood magnitudes directly instead of specific flows. The second part deals mainly with climate change adaptation of Creager curves through correction factors derived utilizing information from current and future period streamflow estimated based on an ensemble of RCM simulations. Details of the study area, observed and modeled data used and detailed methodology are described below.

3.2.1 Study area

The seven major Canadian river basins considered in this study collectively represent a diverse array of topographic, geographical, and hydrological characteristics. Many of these river basins are spread across the Canadian and US territories, but this study focusses only on Canadian parts. The Fraser River basin (231,177 km^2), situated in British Columbia, is characterized by rugged mountain terrain in its upper reaches, gradually transitioning to low-lying floodplains as it approaches the Pacific Ocean and is known for its highly variable precipitation patterns and significant snowpack accumulation in its mountainous regions, influencing its hydrological regime. The Nelson River basin (956,266 km^2), located in Manitoba, is dominated by expansive boreal forests and extensive wetlands. The Mackenzie River basin (1,805,884 km^2), the largest in Canada, spans mostly northern regions, encompasses diverse landscapes such as boreal forests, tundra, and permafrost zones and has a short but intense summer melt season, resulting in significant peak flows. The Yukon River basin (333,397 km^2), primarily located in Yukon and Alaska, features vast wilderness areas, including mountain ranges and boreal forests and is influenced by seasonal ice cover and snowmelt, with peak flows typically occurring in late spring. The Churchill River basin (400,289 km^2), situated in Saskatchewan and Manitoba, traverses varied landscapes ranging from boreal forests to subarctic tundra and is characterized by seasonal ice cover. The St Lawrence River basin (832,133 km^2), encompassing the Great Lakes region, spans several Canadian provinces and US states. Its hydrology is influenced by complex interactions between the Great Lakes, and maritime influences, resulting in diverse flood-generating mechanisms. The St John River basin (35,950 km^2), located in New Brunswick, features diverse landscapes including forested uplands and agricultural lowlands. Its hydrology is influenced by both snowmelt and intense rainfall events, with flood-generating mechanisms varying seasonally (*Core Basins and Observatories - Global Water Futures | University of Saskatchewan*).

3.2.2 Observed and climate model simulated streamflow data

Almost in all engineering projects, design floods are estimated using statistical analysis of peak flows that are derived from continuous streamflow observations available at the site of interest or nearby hydrometric stations. The observed streamflow data considered in this study comes from Water Survey of Canada's hydrometric database, HYDAT, which contains streamflow information at thousands of gauging stations. Although several stations provide instantaneous peak flows, these are generally available for the last quarter of the 20th century and beyond and often contain missing values. Compared to instantaneous peak flows, mean daily flows are available at more stations and for longer periods. The annual maximum values of mean daily flows are hence used in this study for estimating design flood magnitudes, irrespective of the flood generating mechanism. This assumption is justified as the primary interest is on design flood loads the highway bridge is supposed to withstand and not on the time of occurrence of peak flows. A total of 444 HYDAT stations shown in Figure 3.1d, recording natural flows, with at least 20 years of data are considered for the derivation of observed design flood magnitudes and to establish the Creager curve. This long data is generally recommended to obtain robust estimates of flood flow statistics in hydrology (Maidment, 1993; Javelle et al., 2002; Faulkner et al., 2016). Although data from earlier in the 20th century is accessible through HYDAT, this study uses observations collected over the 1951-2020 (70-year) period, with the primary aim of ensuring higher reliability of estimated flood quantiles.

To estimate correction factors to Creager curves, discussed in detail later in this section, current and future period streamflow sequences are derived from Environment and Climate Change Canada (ECCC)'s state-of-the-art RCM GEM (Global Environmental Multiscale) (Côté et al., 1998) simulated runoff, available at 50-km resolution over a pan-Arctic domain (Figure 3.1a), using a modified version of WATROUTE (Soulis et al., 2000; Teufel & Sushama, 2021). An ensemble of five GEM simulations for the 1951–2099 period driven at the lateral boundaries by five different members of a second-generation Canadian Earth System Model (CanESM2) initial condition ensemble, following the Representative Concentration Pathway 8.5 (RCP8.5) scenario are considered. Streamflow is generated at 5-km resolution from the GEM simulated runoff using

WATROUTE, which is a cell-to-cell routing scheme based on the routing algorithm of the WATFLOOD distributed hydrological model (Kouwen et al., 1993) that solves the water balance equation at each grid cell and relates water storage to streamflow using Manning's equation. The flow directions, river lengths and slopes are derived from the HydroSHEDS database (Lehner et al., 2008). The simulated streamflow in current climate have already been validated by comparing against HYDAT observations in Teufel & Sushama (2021), which suggests that the model captures reasonably well the spatial patterns and magnitude of annual maximum streamflow. Timing of peak streamflow occurrence in the model is also found to closely align with observations, typically differing by no more than 6 days. They also reported satisfactory level of agreement between the simulated and observed return levels.

3.2.3 Detailed methodology

Establishment of Creager envelope curves in current climate

For this study, which is focussed on highway bridges at river crossings, 75-year flood magnitude is considered, which is recommended by the Canadian Highway Bridge Design Code (CHBDC). The CHBDC also specifies a design life of 75 years for new bridge structures, unless otherwise approved by the local regulatory authority in the relevant jurisdiction . For any given site, the Creager's equation (Eq. (1)) can be used to derive Creager's coefficient (C) corresponding to the selected design flood. To calculate C value, the flood magnitude corresponding to the 75-year return period is used, which is obtained by frequency analysis of annual maximum mean daily streamflow values, to be discussed later in this section. Computation of design floods corresponding to higher return periods requires longer records. Roughly, $2T$ rule, where T is the return period, is recommended (Robson & Reed, 1999) i.e., data records twice as large as the return period of interest. According to this recommendation, a minimum of 140 years of data is required to estimate the 75-year flood. The HYDAT stations selected for this study have a mean record length of 48.72 years, and therefore no station alone satisfies this criterion (Figure 3.1d). Since the observational data is not continuous in time and space, regional frequency analysis (RFA) approach of Hosking & Wallis (1997) using the concept of statistical homogenous regions is used to estimate desired design floods. The RFA approach compensates time with space and thus helps in estimating robust design floods at sites which lack sufficient data. The index flood procedure (Dalrymple, 1960) is the basis for the RFA approach used in this study. This approach was formalised by Hosking & Wallis (1997) based on L-moments. Analogous to conventional moments, L-moments are linear combinations of order statistics and are considered to be more robust to extraordinary large values (i.e., so called outliers) in a given sample of peak flows compared to the conventional moments. L-moments can be used to estimate parameters of many statistical distributions that are commonly used in FFA. Details can be found in Hosking & Wallis (1997).

For applying RFA, it is important first to identify homogeneous regions or evaluate homogeneity of preconceived target regions of interest or groups of stations. The statistical homogeneity can be verified using different methods, some of which are the Dalrymple test (Dalrymple, 1960), CV-test (Lettenmaier et al., 1987), S-test (Pilon et al., 1991), R-test (Wiltshire, 1986), and the most commonly used H-test (Hosking & Wallis, 1997). This study uses the H-test to evaluate statistical homogeneity of target regions of interest. This test compares the between site variations in sample L-moment ratios (i.e., L-coefficient of variation (L-CV), L-skewness and L-kurtosis) with the expected variations for a homogeneous region. This is accomplished using repeated Monte-Carlo simulations of a homogenous region with the same record length for each site as the observed

(Hosking & Wallis, 1997). The simulation procedure is assisted with a Kappa distribution fitted using regionally averaged sample-size weighted L-moment ratios. To eliminate errors associated with discordant sites, the data is screened using a discordancy measure (Hosking & Wallis, 1997). Based on the outcomes of simulation experiments, three measures of heterogeneity can be defined i.e., H1, H2 and H3 corresponding respectively to L-CV, L-skewness, and L-kurtosis. If $H < 1$, the region is considered acceptably homogenous, possibly homogenous for values between 1 and 2 and heterogeneous if $H > 2$. Detailed procedure along with mathematical formulations is available in Hosking & Wallis (1997) and a brief description is provided in the appendix of this paper. Heterogeneous regions need to be subdivided into smaller regions, which can be done by using cluster analysis algorithm described in Hosking & Wallis (1997), by subjective or objective partitioning based on geographic proximity or by invoking homogeneity of regional climate and environmental factors such as climatic regions.

Homogeneity analyses are performed at the level of individual basins. Given the size and geographical extent of these basins, the flood generating mechanisms and catchment characteristics might vary within the same basin. This is expected especially for larger basins like Mackenzie River basin. Where applicable, this study also uses a logical partitioning of larger basins based on the influence of 11 climatic regions (Plummer et al., 2006; ECCC, 2023) to further divide them into smaller regions to ensure similarity of both climatic and flood characteristics to support sensible RFA (Mladjic et al., 2011).

The next step involved in RFA is the selection of a regional distribution. Previous studies in Canada have considered the generalized extreme value (GEV), three-parameter lognormal (LN3), generalized normal (GNO), log-Pearson Type III (LP3) and Pearson Type III (PE3) distributions for FFA (Yue & Wang, 2004; Aucoin et al., 2011; Clavet‐Gaumont et al., 2013; Huziy et al., 2013; Yang, 2016). Based on goodness-of-fit analysis following the Z-test of Hosking & Wallis (1997), aided with L-moment ratio diagrams and the recommendations of previous studies, the GEV distribution is selected for this study. This choice is also consistent with theoretical arguments i.e., the distribution of maxima of a sample of independent and identically distributed random variables converges to the GEV distribution (Coles et al., 2001). Parameters of the GEV distribution for each region are estimated by equating the sample size weighted average values of sample L-moment ratios to their theoretical counterparts and solving the resulting equations. Desired design floods at a given site in each region are estimated using quantiles from the regional growth curve, that represents a dimensionless relationship between frequency and magnitude, and at-site index flood, which is taken as the mean annual flood. Estimated design floods are then used in the Creager's equation (Eq. (1)) to estimate values of C for all sites in a region.

Climate change adaptation of Creager envelope curves for future climate

The second part of the proposed framework is related to adapting the Creager curves (i.e., C values) to changing design floods in future climate. It is proposed here, to apply correction factors, defined as $R_c = C_f/C_p$, where C_f and C_p are respectively the Creager coefficients for the future and current time periods, to the design values obtained from HYDAT-based observations presented above in the first part of the framework. Design flood magnitudes for the current/reference 1951–2020 period and targeted future time periods are estimated at observation sites from transient climate change simulations in a similar manner as described above for observed floods. The values of C for the current and future time periods can also be derived in a similar manner as described above. Any model biases present in both current and future period climate model simulations are assumed to cancel out and, hence, will not affect the climate change signal (Hay et al., 2000; Beniston et al., 2007; Fowler & Ekström, 2009; Mladjic et al., 2011). This ratio can then be applied as a correction factor.

Five members of the Canadian Earth System Model (CanESM2; Arora et al. (2011)) driven GEM simulations for the period 1951–2020 are considered as the reference current climate simulations. The future period corresponds to 2021–2099 for each of the ensemble member; using the 70-year window as in current climate, 10 future periods are considered from the 2021–2099 using a moving window approach. The 75-year design flood is calculated for both current and future periods using two RFA approaches, considering the same regions as identified in the first step of RFA using observational data, described above in this section. In the first RFA approach, for a given region, only streamflow at grid cells where the observation stations are located are considered. In the second approach, streamflow at all grid cells of a given region are considered for RFA.

The confidence in R_C is assessed in terms of coefficient of variation, defined as the ratio of the standard deviation to the ensemble average obtained from the five pairs of simulations. The confidence in the projected changes is considered high if the coefficient of variation is small. This approach has been adopted before in several studies (e.g., Mladjic et al. (2011), Khaliq et al. (2015), PaiMazumder & Done (2014), Qian et al. (2020)).

3.3 Results and discussion

3.3.1 Derivation of Creager curves and coefficients from observational data

Before conducting RFA to estimate desired flood magnitudes at various locations within the seven large river basins, homogeneity analysis, as described in the methodology section, is conducted at the level of individual basins. The results of this analysis exhibit significant variability in the values of homogeneity measures for the study region, with values exceeding 3 for most of the basins. This lack of homogeneity can primarily be attributed to variations in flood flow statistics, distinct flood mechanisms and diverse terrain characteristics and thus necessitates further subdivisions of the selected basins into logical partitions by invoking characteristics of the associated controlling climate than merely depending on statistical measures of homogeneity to support implementation of the RFA approach. To garner the advantages of RFA together with the homogeneous features of Canadian climatic regions, sub-basins within each major river basin are grouped into smaller regions based on the specific climatic zones they are situated in. This approach aims to account for the unique sub-basin characteristics and heterogeneity challenges of large river basins, potentially leading to a more logical approach from a climate perspective for conducting region-specific FFA. The HydroSHEDS data (Lehner et al., 2008) is utilized to identify sub-basins for creating within-basin groupings. Among the seven river basins, Fraser, Yukon, St John and Churchill are retained in their original form due to their marginal departures from statistical homogeneity measures. However, the Mackenzie River, Nelson River and St Lawrence River basins are subdivided into 10, 3 and 2 sub-regions, respectively (Table 3.1). This subdivision resulted in a total of 19 regional partitions of the study area, shown in Figure 3.1c, that serve as the basis for RFA, allowing for a better strategy to address the diversity of flood flow characteristics and variations in landscape features. It should be noted that the homogeneity measures of these regions do not completely satisfy the criteria set by Hosking & Wallis (1997), however, dividing these regions further would reduce the availability of observational data to support a sensible RFA. There is a trade off between achieving absolute homogeneity by reducing number of stations and having enough stations to support a reliable RFA. The identified 19 regions are therefore assumed reasonable to achieve the objectives of this study.

Using these 19 regions as the basis for RFA, 417 stations that passed the discordancy test are used to estimate 75-year design floods using the method of L-moments and the GEV distribution (Figure 3.2a), and the corresponding C values derived from the Creager's equation for each of the station points falling within the seven basins are aggregated and shown in the form of boxplots in Figure 3.2b. The values of C obtained for each station for the study region (Figure 3.2c) show a considerable spread, ranging from 0.2 to 45. As expected, the relatively drier regions of central Canada have considerably lower values of C compared to the rest of the study area, and the regional maximum values range from 4 to 10 in these regions, whereas it is higher for sub-regions of Mackenzie and Yukon River basins with values as high as 45 and 30 respectively (Figure 3.2d). The Creager curve for any region is generally created using only the maximum values as a function of drainage area, so that it encompasses all points within it. Consequently, it is likely that within these larger basins, the Creager's envelope curve created for the highest flood value will likely result in a significant overestimation of the same at stations with lower drainage areas. To summarize estimated values of C, Table 3.2 shows the maximum, minimum and mean values of C for each basin as a function of different ranges of drainage area. The results shown in this table emphasize the need to consider the scale of basin drainage area for better interpretation of C values to prevent overestimation of design floods. It can be seen that even for stations with similar drainage area within larger basins, the variability in C values are high. This wide range of C values underscore the complexity of hydrological processes and flood behaviors, emphasizing that drainage area alone may not fully explain the observed differences in flood characteristics and severities. For the Churchill and Nelson River basins, addition of more stations or sub-basins with larger drainage areas than considered in this study may increase the range of C values for those categories of drainage area.

The values of C obtained using the annual maximum mean daily flows are expected to be lower than those obtained using the instantaneous peak flows. However, for the purpose of this study and to establish a framework for developing changes to design flood values, it is assumed that the behavior of instantaneous peak flow may experience a similar type of change as the annual maximum mean daily flow. While the absolute values of C may differ between the two data types, the relative changes in C values can still provide valuable insights into the potential changes that the design floods may undergo as a consequence of future climate change. This assumption allows for a meaningful analysis and development of a practical approach for gauging existing design standards and guidelines in the context of this study, even if it doesn't capture the full range of variations of instantaneous peak flows.

3.3.2 Creager curve correction factors to represent future design floods

The first step in the estimation of R_C is the selection of an appropriate future time window that is comparable with the time window of the current reference period (i.e., 1951–2020). As explained in Section 3.32, R_C is then estimated as the highest ratio of future to current C values obtained using a moving window of 70 years over the 2021–2099 period, which yields 10 different future time periods starting from 2021–2090 and going up to 2030–2099.

Results based on the first RFA approach are presented first, followed by those of approach 2. The maximum value of R_C obtained for each of the 19 regions are mostly for the end-of-century time window i.e., 2030–2099. Certain regions, especially those in central Canada, show $R_C < 1$ moving further into the future. This could be due to the projected decrease in streamflow into the future, compared to other regions. The projected changes to the 75-year design flood for each of the five members in the ensemble and the corresponding ratio, R_C is shown in Figure 3.3.

The projected changes to design flood and the values of R_C for grid cells corresponding to observation stations within each river basin are calculated using ensemble averaged values for the selected future time periods and are shown in Figure 3.4a. The simulated streamflow sequences for each of these grid cells represent integrated response of the upstream catchment area. Spatial patterns of R_C values indicate that the larger decreases are more prominent in the south-eastern regions and prairies. The evaluation of confidence in the R_C is studied by analyzing within ensemble variability utilizing coefficient of variation (the ratio of standard deviation to the ensemble-mean of R_C). Smaller the value of this measure, the higher will be the level of confidence in R_C. The values of coefficient of variation for observation points, shown in Figure 4b based on five pairs of current and future period simulations, are small over most parts of the study region, with slightly higher values observed for some points in the southern parts of the Nelson River and St Lawrence River basins.

These values for each river basin, organized into five different categories of drainage area, are presented in Figure 3.5a. Additionally, Figure 3.5b consolidates all these values for each river basin and provides an overview of the range of R_C in the form of boxplots. These figures offer a visual representation of the distribution and comparison of summary statistics of the values across all basins and drainage area categories. Both increases and decreases can be observed within each basin, with the highest R_C (reflecting highest relative increase in the design flood) observed for the Nelson River (1.54), Mackenzie River (1.26) and Yukon River (1.37) basins. The projected value of R_C for 24.5% (102 out of 417) of station points is greater than 1.0. Churchill River and Mackenzie River basins have the largest number of stations/grid points, respectively 70.4% and 43.8%, showing an increase. These results highlight the spatial diversity in how climate change is expected to impact design flood levels and flood risk across different station points within each basin. Among all basins, both the St John River basin and the St Lawrence River basin consistently exhibit decreasing C values across all drainage area categories with no station point showing an increase in the former basin and only one instance of increase in the latter basin. In these regions, it can reasonably be assumed that the existing design guidance and standards may not require revisions to account for future climate change. The substantial decreases in C values also suggest that the current design guidelines are likely to overestimate the design flood loads, making them more conservative than necessary. In contrast, for all other regions with $R_C > 1$ indicate a need to revise design guidance and existing Creager curves. It is also worth noting that for the Nelson River and Yukon River basins, that show considerable increases in the projected design flood loads, for headwater basin areas, with lower drainage areas, the C value is projected to decrease. In such regions, adopting different C values for different basin areas within the larger basin seems reasonable. Flood envelope curves, using historical data and after applying R_C to reflect future curves, for different drainage area categories, are shown in Figure 3.6. It should be noted that an envelope curve for a region that have insufficient number of stations within a drainage area category might underestimate the peak flood and is not considered.

It is essential to acknowledge that the results presented are constrained by the availability of station points. To further evaluate potential disparities that may arise when ungauged locations are also considered, approach 2 is used. Results obtained with approach 2 suggest similar results over the study domain with larger decreases more prominent in southern regions of Canada. About 32.89% of grid cells in the study region have $R_C > 1$.

The values of R_C corresponding to the observation points considered in approach 1 for each river basin, categorized based on five distinct drainage area classes (Table 3.3), are illustrated in Figure

3.7a. Furthermore, Figure 3.7b presents a summary of these values for each river basin separately. The projected changes to design flood and the R_C values for all grid cells are shown in Figures 8a and 8b respectively and the region averaged values of R_C is shown in Figure 3.8c which shows considerable differences in the magnitude and spatial patterns. The projected changes to design flood and R_C values for each member of the ensemble are given in Figure S1 (supplementary material). Comparison of these results with Figure 3.4a suggests that the inclusion of additional points helped uncovering additional insights such as widespread increases in all regions within the study domain, with the western areas displaying the most significant disparities in spatial patterns and elevated R_C values. In contrast, the prairies and south-eastern regions exhibit more prevalent decreases in both spatial patterns and R_C values. A comparison of the regional growth curves for the 19 regions, for each of the five members of the simulation for the present and future time periods can be seen in Figures S2 and S2 (supplementary material). Figure 3.8d shows the coefficient of variation of R_C indicating that, apart from the southern parts of the Nelson River basin, the rest of Canada exhibits lower values that consistently remain below 1 across the entire domain.

3.4 Summary and conclusions

A framework for updating current flood envelope curves by developing correction factors to reflect future changes to design floods is proposed in this study, by focussing on seven major Canadian river basins that cover most of Canada. Firstly, observed values of the Creager's coefficient are calculated using design flood magnitudes, assumed to be 75-year flood, obtained through RFA of annual maximum mean daily flows, sourced from the HYDAT database of ECCC for the period 1951–2020.

The correction factor R_C is then determined using two approaches based on a five-member ensemble of streamflow simulations spanning the 1951–2099 period, generated using an integrated climate-hydrology regional climate modeling system. The first approach estimates R_C at observation sites as the ratio of future to current C values, where the future and current design flood values are estimated using RFA approach by considering only the 5 km grid cells where the observation stations are located. The second approach is similar to approach 1, except that it considers all grid cells of a given region in the RFA approach to estimate future and current design flood magnitudes. The use of five-member ensemble in both methods enabled quantification of uncertainty in estimated R_C values.

The following key findings can be inferred from the analyses presented in this paper:

1) The seven selected large river basins do not meet the required statistical homogeneity criteria set by Hosking & Wallis (1997) for their direct use in RFA. However, by dividing large river basins into sub-basins based on Canadian climatic regions they are in, relatively more accurate estimates of design floods using the RFA approach are obtained. It is important to note that the 19 subregions used in the study can potentially be further subdivided into smaller, relatively more homogenous regions to refine the analysis, but will be unable to facilitate adequate observational data to support a reliable RFA.
2) The values of Creager's coefficient derived from observations exhibit significant variations across the study region, ranging from less than 1 to more than 40, with the highest values noted for the Mackenzie River basin (~ 45). This variability can be attributed to the diverse climate, landforms and geographic controls that impact flood generating mechanisms in different parts of the study domain. In general, instantaneous peak flows are used to develop Creager curves, however, for the purpose of this study, annual maximum mean daily flows are considered.

Longer time series of mean daily flows are more frequently available than that of instantaneous peak flows. It is important to acknowledge that Creager's coefficient calculated using instantaneous peak flows will likely be higher than the values derived from mean daily flows. While the absolute values of C may differ between the two data types, the relative changes in C values can still provide valuable insights into the potential changes that the design floods may undergo because of future climate change.

3) The ratio R_C shows values above and below one over the study domain, with 24.5% of observation stations likely to have $R_C > 1$. For the Churchill River basin, $R_C > 1$ is noted for 70% of stations, while St John River basin generally shows $R_C < 1$. A quantification of the spread of R_C values based on the five pairs of current and future period simulations, represented in the form of coefficient of variation, suggest higher confidence for most parts of the study domain, except parts of the Nelson River and St Lawrence River basins.
4) Incorporation of simulated streamflow data for ungauged locations, specifically by using all grid cells of a region, can offer an effective approach to mitigating the impacts of data availability constraints. This methodology when applied reveals most of the study region to undergo projected decreases in design flood values, with $R_C > 1$ for 32.89 % of grid cells, with higher increases in western Canada. Thus, this strategy can help understand flood loadings on infrastructure assets in ungauged areas.
5) Finally, the study offers valuable insights into determining changes to design flows and their quantification in terms of correction factors for Creager coefficient, which are essential for the development and planning of climate adaptation strategies.

It is crucial to recognize that the findings of this study are based on transient climate change simulations from a single RCM and employing a single emission scenario. To account for model and emission scenario related uncertainties, additional models and emission scenarios must be considered in the future. As such, the study provides a science-informed logical framework for updating flood envelope curves, which are commonly used by practitioners in estimating design flood magnitudes, to factor in climate change. Future research should consider performing a similar analysis, by directly considering model simulated instantaneous peak flows or by converting mean daily flows to instantaneous peak flows using appropriate methods such as those included in (Sangal, 1981), (Chen et al., 2017) and (Khaliq, 2023). The outputs of such a study are expected to complement and strengthen the findings reported herein. On the climate modeling aspects, we believe physics informed machine learning and deep learning approaches for generating high-/super-resolution climate model outputs (e.g., (Teufel & Sushama, 2022), (Kashinath et al., 2021)) will be useful for generating large ensembles to better quantify uncertainties. Such approaches should be explored in the future using modern machine learning architectures and physically consistent simulation frameworks (Vadyala et al., 2022). Additionally, machine learning approaches should also be explored to improve predictive maintenance of engineering infrastructures (Scaife, 2023).

Acknowledgements

The GEM simulations considered in this study were performed on supercomputers managed by the Digital Research Alliance of Canada and Calcul Québec. This research was funded by the National Research Council of Canada (through the Climate-Resilient Built Environment initiative) and Trottier Institute for Sustainability in Engineering and Design. The helpful comments of the editor and two anonymous reviewers are very much appreciated.

Appendix

L-moment ratios

Analogous to conventional product moments, L-moments are also used to fit and describe the shape of a probability distribution Hosking & Wallis (1997). Nearly for all applications, the following equations are used to calculate the first four sample L-moments in terms of probability weighted moments (b_r) for a site with n observations:

$$l_1 = b_0 \tag{A1}$$

$$l_2 = 2b_1 - b_0 \tag{A2}$$

$$l_3 = 6b_2 - 6b_1 + b_0 \tag{A3}$$

$$l_4 = 20b_3 - 30b_2 + 12b_1 - b_0 \tag{A4}$$

The probability weighted moment b_r of order r is given by:

$$b_r = n^{-1} \sum_{j=r+1}^{n} \frac{(j-1)(j-2)\dots(j-r)}{(n-1)(n-2)\dots(n-r)} x_{j:n} \tag{A5}$$

where $x_{j:n}$ are the ordered sample values. L-moment ratios are dimensionless versions of L-moments and are defined as:

$$t_2 = l_2/l_1 \text{ (L-CV)} \tag{A6}$$

$$t_3 = l_3/l_2 \text{ (L-skewness)} \tag{A7}$$

$$t_4 = l_4/l_2 \text{ (L-kurtosis)} \tag{A8}$$

The regional average L-moment ratios for a region *R* with *N* sites, with respective sample sizes n_1, n_2,.., n_N are then given by:

$$t_r^R = \frac{\sum_{i=1}^{N} n_i t_r}{\sum_{i=1}^{N} n_i}, r = 2, 3, 4 \tag{A9}$$

Hosking & Wallis (1997) introduced a discordancy measure D_i to identify grossly discordant sites from the whole group of sites, measured in terms of the L-moments of the data to screen out sites with gross errors.

If $\boldsymbol{u}_i = [t_2^{(i)}, t_3^{(i)}, t_4^{(i)}]$ be the vector containing the L-moment ratios of site i and $\bar{\boldsymbol{u}}$ is the vector of unweighted regional average L-moment ratios, the discordance measure for site i is defined as:

$$D_i = \frac{1}{3}(\boldsymbol{u}_i - \bar{\boldsymbol{u}})^T \boldsymbol{A}^{-1}(\boldsymbol{u}_i - \bar{\boldsymbol{u}}) \tag{A10}$$

where $\boldsymbol{A}$ is the sample covariance matrix, defined as:

$$\boldsymbol{A} = (N-1)^{-1} \sum_{i=1}^{N} (\boldsymbol{u}_i - \bar{\boldsymbol{u}})(\boldsymbol{u}_i - \bar{\boldsymbol{u}})^T \tag{A11}$$

and T denotes transpose of a vector or matrix.

Regional heterogeneity measures

Hosking & Wallis (1997) proposed a statistical test for testing the homogeneity of a given region. This test compares the between-site variation in sample L-moment ratios with the expected variation for a homogeneous region. Supposing that the selected region has N sites, with the ith site having a record length of n_i and t_r^R as defined above, the following V and H statistics are calculated for the region,

$$V_k = \left[\sum_{i=1}^{N} \frac{n_i\left(t_r^{(i)} - t_r^R\right)^2}{\sum_{i=1}^{N} n_i}\right]^{\frac{1}{2}}, r = 2, 3, 4; k = 1, 2, 3 \tag{A12}$$

$$H_k = (V_k - \mu_{V_k})/\sigma_{v_k} \tag{A13}$$

The statistics V_1, V_2 and V_3 respectively correspond to L-CV, L-skewness and L-kurtosis. H_k is a measure of the variability of L-moment ratios in the region compared with that expected for simulated homogeneous regions; μ_{V_k} and σ_{V_k} are the expected mean and standard deviation of the variability measures for a homogenous group of sites, estimated through repeated Monte Carlo simulations. Interpretation of H_k values is provided in the main text and additional details on the above procedures and mathematical formulations can be seen in Hosking & Wallis (1997).

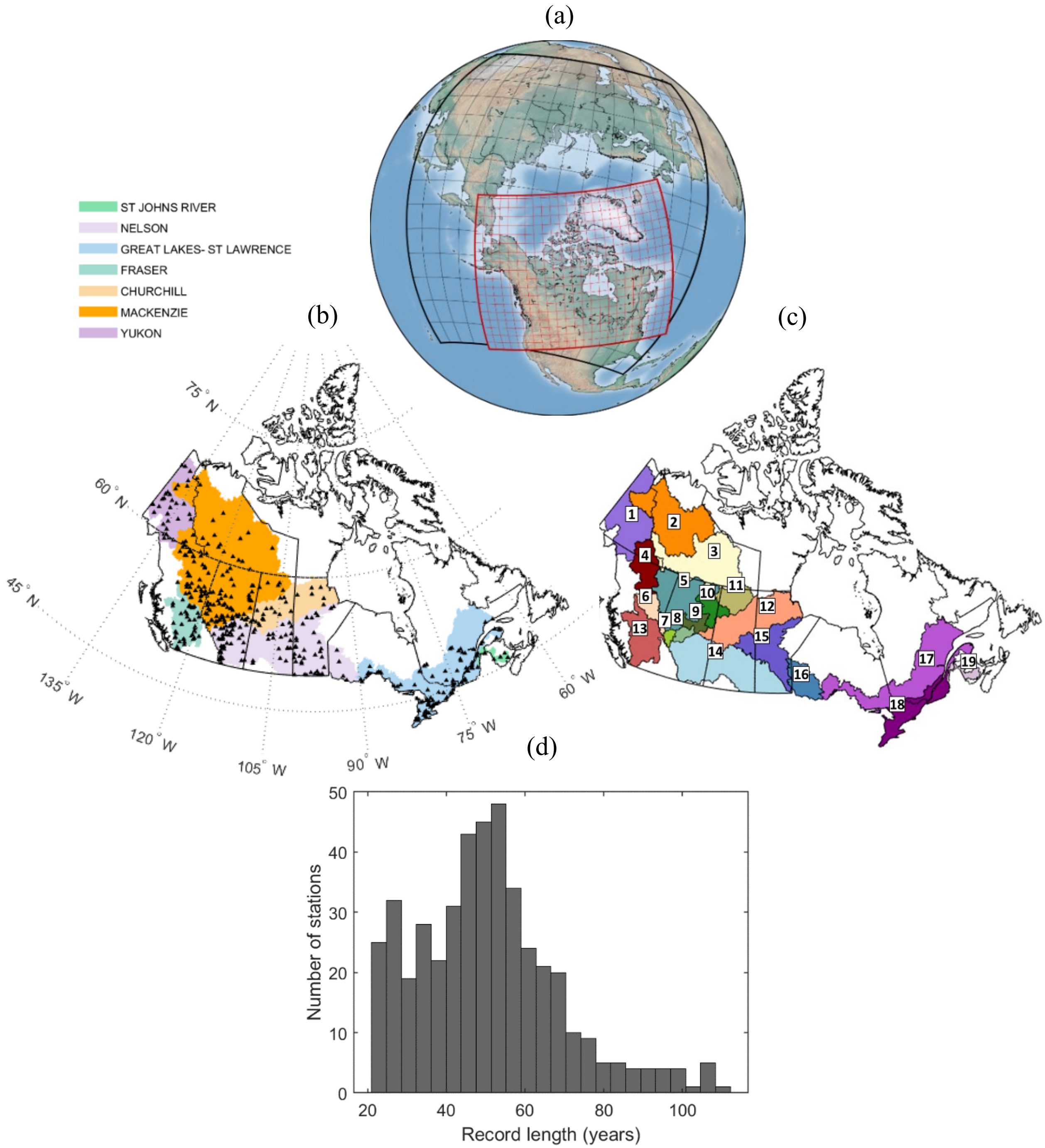

Figure 3.1(a) GEM and WATROUTE experimental domain at 50-km (in black) and 5-km (in red) resolutions; gridlines correspond to every 15th and 50th grid point respectively. **(b)** Map of Canada showing the seven major river basins and observation sites (black triangles). **(c)** Nineteen sub-regions (labeled as 1–19) considered within the seven large river basins to support RFA. **(d)** Distribution of observed record length for the 444 HYDAT stations selected for the study.

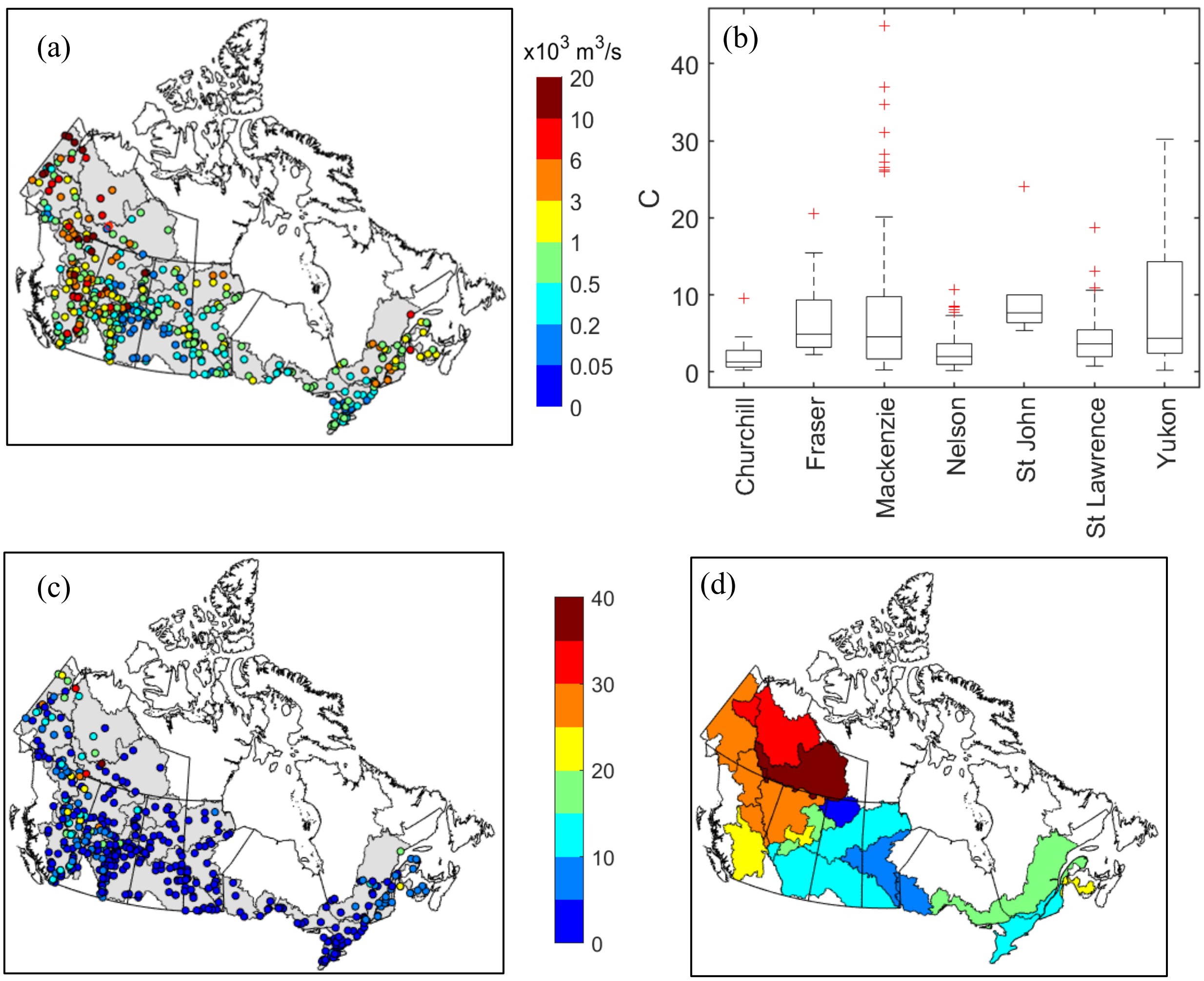

Figure 3.2 (a) 75-year design flood value shown at the level of individual HYDAT stations within the study domain calculated using observation data and the RFA approach. **(b)** Boxplots illustrating basin-level summary statistics of the Creager coefficient C based on the 75-year design flood values. The box in each boxplot displays the 25th, 50th and 75th percentile values; the whiskers extend to 1.5 times the interquartile range (75th–25th percentile values) from the respective (lower/upper) end of the box; and outlying points show the values which are considerably different than the rest (Helsel & Hirsch, 2002) **(c)** Creager coefficient (*C*), shown at the level of individual HYDAT stations within the study domain, calculated using observation data. **(d)** The maximum value of *C* obtained from observation stations within each of the 19 regions, represented by a single color for a region.

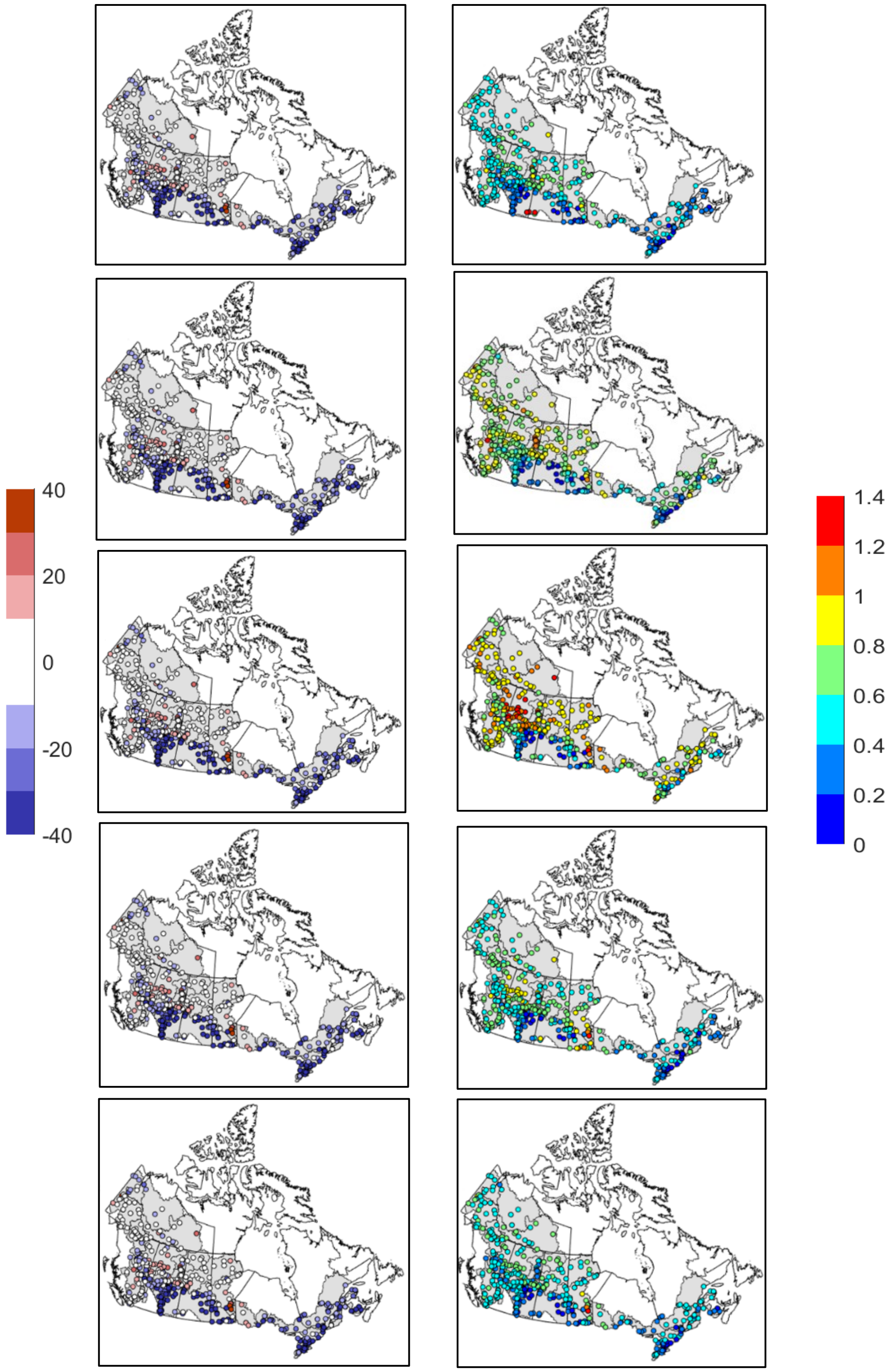

Figure 3.3 Projected changes to 75-year design flood (in percentage) shown at the level of individual HYDAT stations (approach 1) within the study domain (left panel) and the respective calculated value for the ratio R_C (right panel) for each of the five members in the ensemble.

(a)

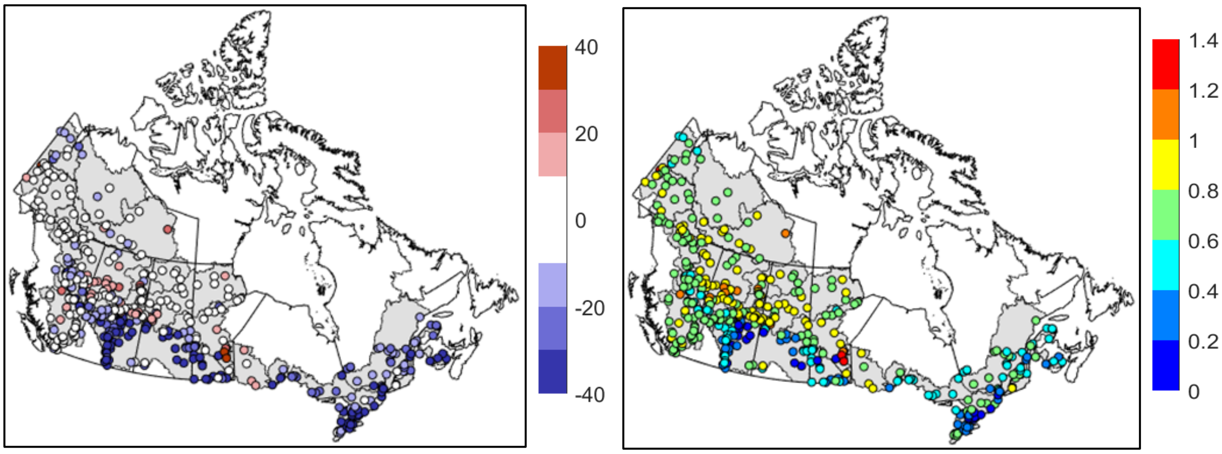

(b)

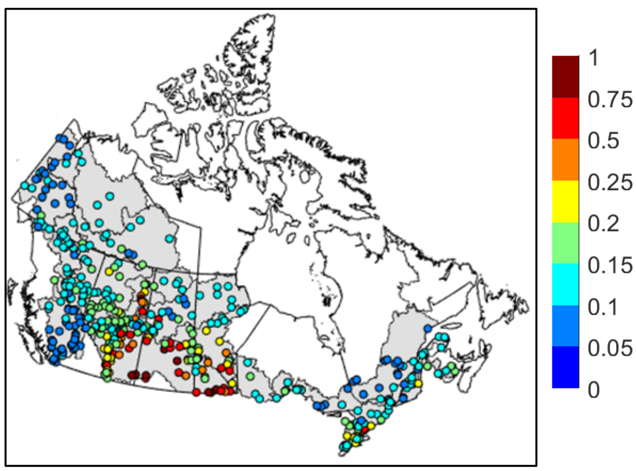

Figure 3.4 (a) Ensemble averaged projected changes to 75-year design flood values in percentage (left panel) and ensemble averaged R_C (right panel) shown at the level of individual HYDAT stations (approach 1) within the study domain. **(b)** Coefficient of variation of R_C based on five pairs of current and future period simulations.

(a)

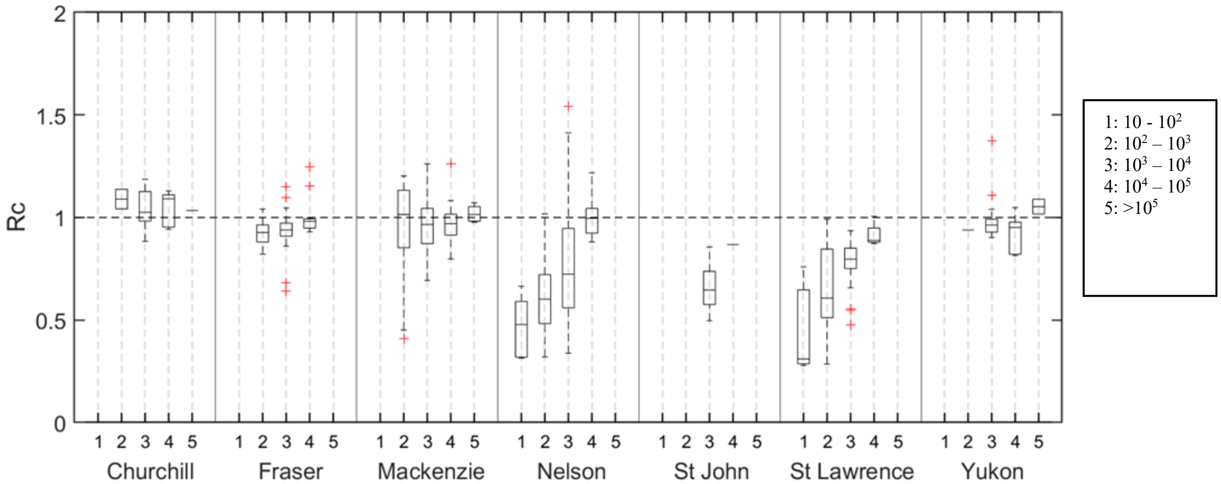

(b)

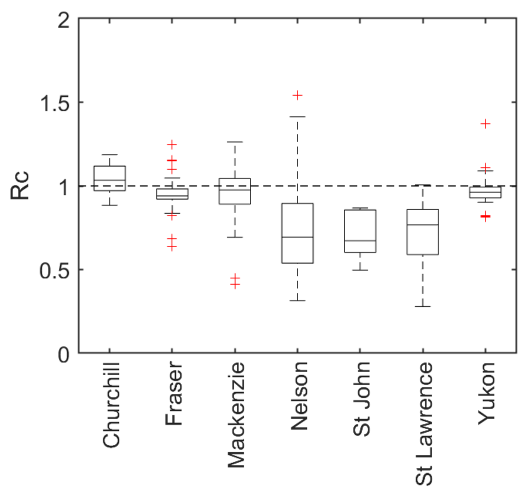

Figure 3.5 (a) Boxplots of R_C values, calculated using approach 1, grouped based on five categories of drainage area (in km^2) within each of the seven basins. **(b)** Boxplots illustrating variations in the values of R_C for each of the seven basins, considering the entire basin as a single entity. Description of boxplots is provided in Figure 3.2.

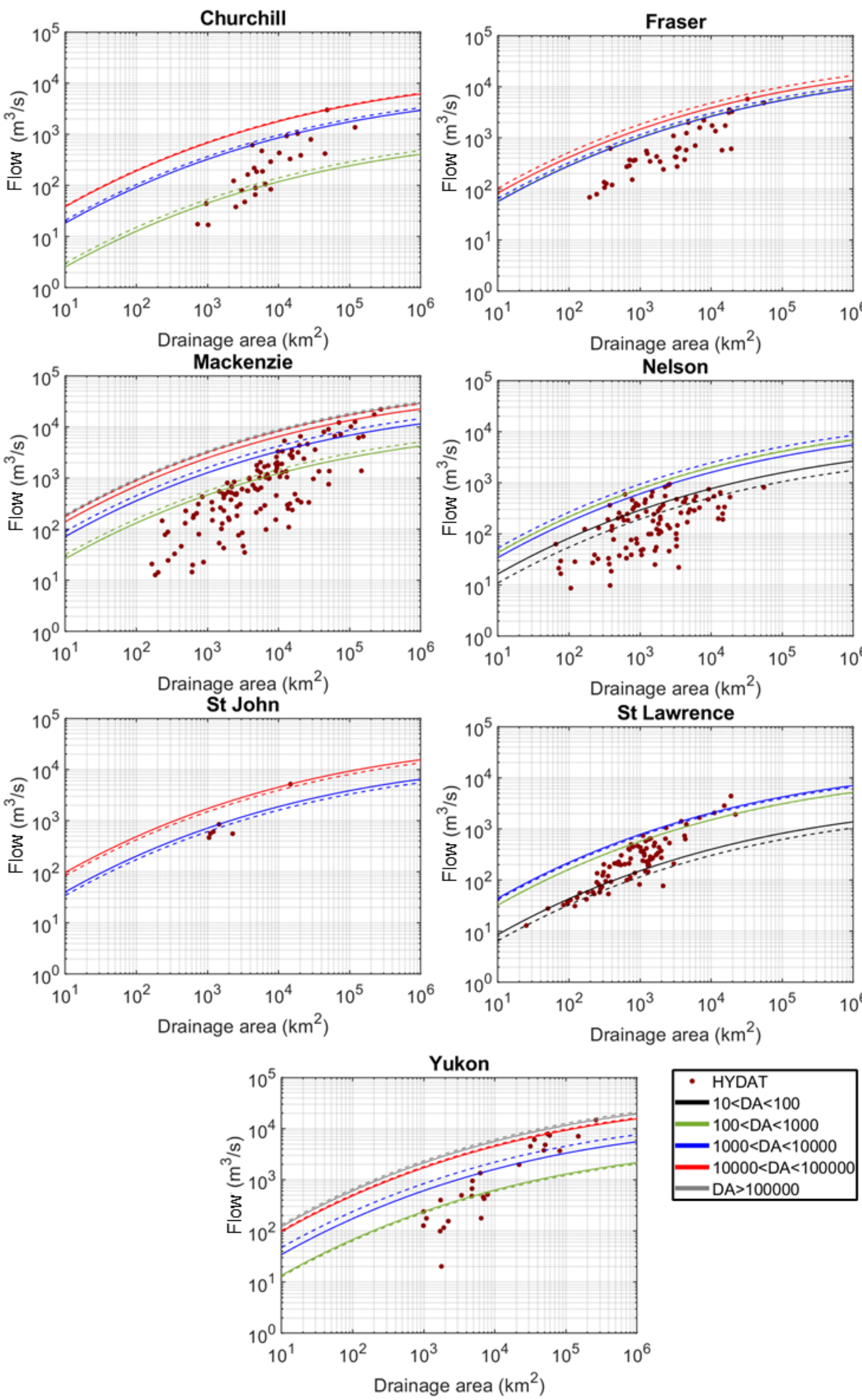

Figure 3.6 Creager curves for all seven river basins constructed using C values from observations (full lines) and corrected C values (dotted lines) using the maximum value of R_C for each drainage area (DA) category, represented by different colors. The points correspond to the 75-year design flood value calculated from observations.

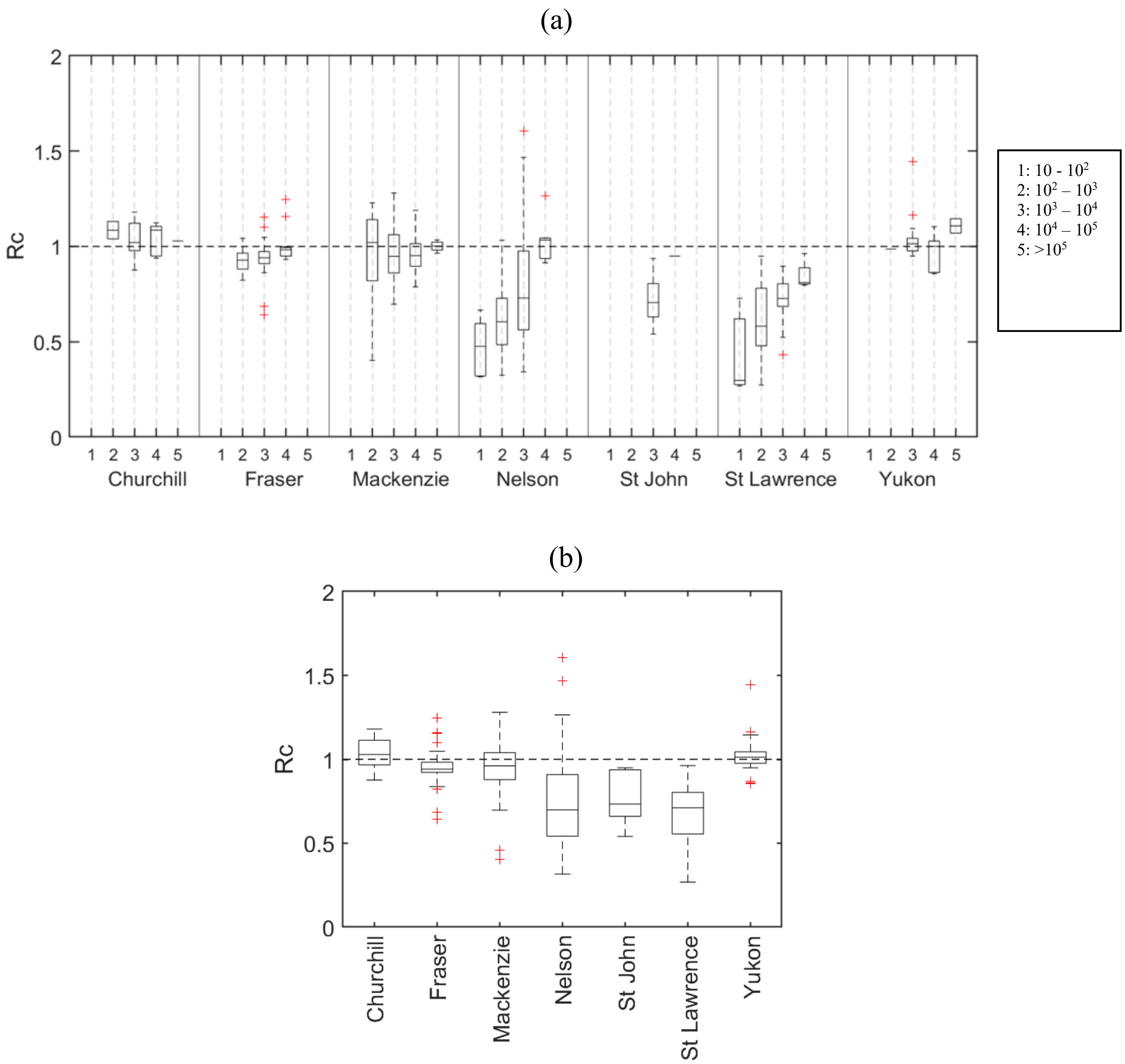

Figure 3.7 (a) Boxplots of R_C values at the HYDAT stations, calculated using approach 2, grouped based on five categories of drainage area (in km^2), shown in the legend, for each of the seven river basins. **(b)** Boxplots illustrating variations in the values of R_C, calculated using all grid cells for each of the seven river basins, considering the entire basin as a single entity. Description of boxplots is provided in Figure 3.2.

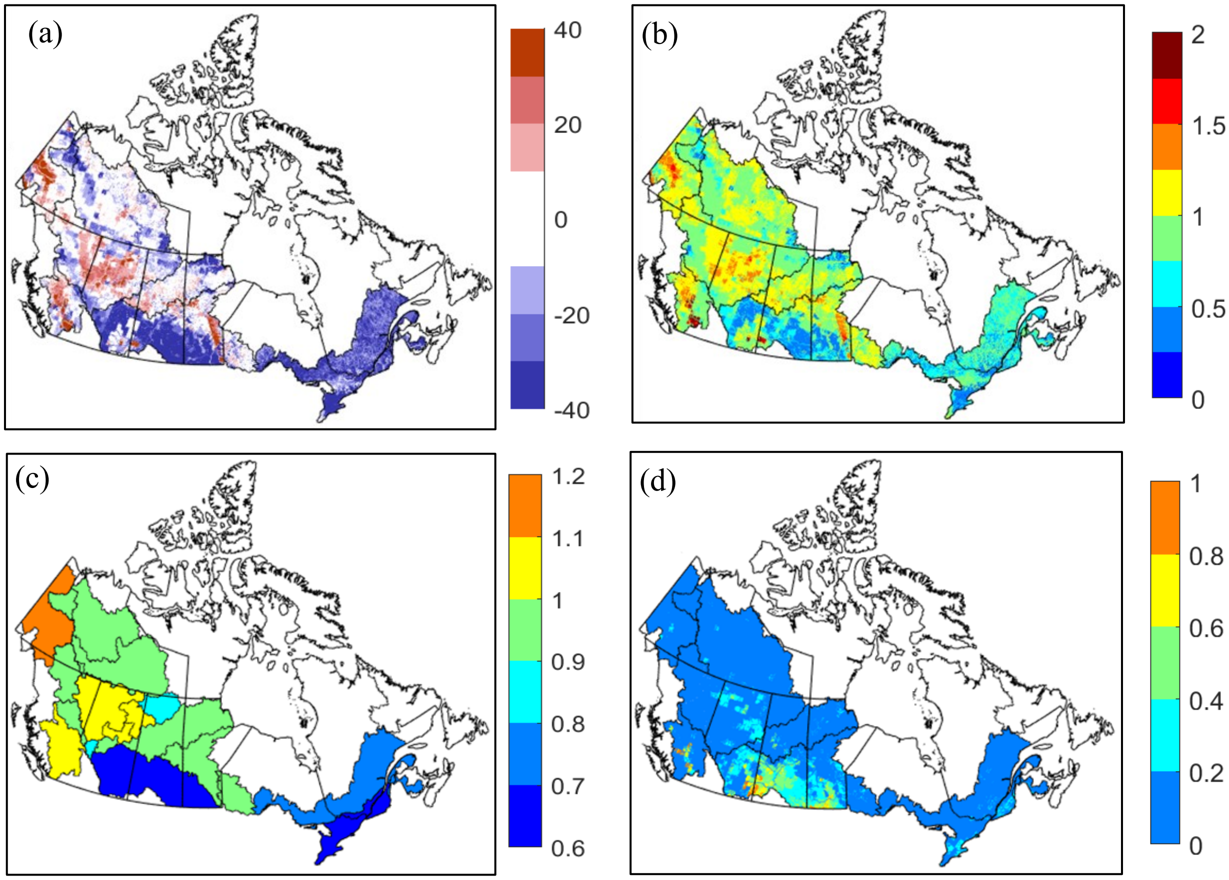

Figure 3.8 (a) Ensemble average of the projected changes to 75-year design flood (in percentage). **(b)** Ensemble mean values of R_C, shown at the level of each grid cell within a region. **(c)** Region-averaged ensemble mean values of R_C, calculated using approach 2. **(d)** Coefficient of variation of R_C based on five pairs of current and future period simulations.

Table 3.1 Large basin partitions and number of observation stations associated with each of the 19 regions/sub-regions used in RFA.

River basin	Sub-region	No. of stations
Yukon	1	27
Mackenzie	2	19
	3	8
	4	13
	5	14
	6	5
	7	10
	8	6
	9	12
	10	11
	11	31
Churchill	12	27
Fraser	13	43
Nelson	14	75
	15	4
	16	21
St Lawrence	17	37
	18	49
St John	19	6

Table 3.2 Creager's coefficient C for the selected seven river basins for various categories of drainage area, along with number of available stations

River basin	Drainage area category	No. of stations	C values		
			Maximum	Mean	Minimum
Churchill	100-1000	2	0.63	0.46	0.29
	1000-10000	16	4.55	1.24	0.24
	10000-100000	8	9.53	3.53	1.36
	>100000	1	3.40	3.40	3.40
Fraser	100-1000	13	14.07	4.60	2.29
	1000-10000	19	14.01	5.99	2.25
	10000-100000	11	20.57	11.11	2.59
Mackenzie	100-1000	20	6.55	2.19	0.26
	1000-10000	66	17.80	5.30	0.29
	10000-100000	34	34.67	10.80	0.52
	>100000	7	44.87	24.61	3.26
Nelson	10-100	4	4.90	2.03	0.98
	100-1000	36	10.64	3.00	0.23
	1000-10000	51	8.54	2.65	0.18
	10000-100000	9	3.11	1.88	0.90
St John	1000-10000	5	10.00	7.43	5.38
	10000-100000	1	24.08	24.08	24.08
St Lawrence	10-100	5	2.13	1.86	1.61
	100-1000	40	8.05	3.36	1.16
	1000-10000	37	10.95	4.95	0.77
	10000-100000	4	18.75	12.56	7.82
Yukon	100-1000	2	3.36	2.58	1.79
	1000-10000	15	8.60	3.19	0.22
	10000-100000	8	24.14	16.12	8.06
	>100000	2	30.20	23.42	16.64

Table 3.3 Changes in the Creager's coefficient C expressed as the ratio R_C for different river basins and drainage area categories as well as corrected values of C.

River basin	Drainage area category	No. of stations	R_C			Corrected C		
			Maximum	Mean	Minimum	Maximum	Mean	Minimum
Churchill	100-1000	2	1.14	1.09	1.04	0.72	0.50	0.30
	1000-10000	16	1.19	1.04	0.88	5.40	1.29	0.21
	10000-100000	8	1.13	1.04	0.94	10.76	3.68	1.29
	>100000	1	1.03	1.03	1.03	3.51	3.51	3.51
Fraser	100-1000	13	1.04	0.93	0.82	14.65	4.26	1.88
	1000-10000	19	1.15	0.93	0.64	16.13	5.58	1.44
	10000-100000	11	1.25	1.01	0.93	25.66	11.21	2.41
Mackenzie	100-1000	20	1.20	0.96	0.41	7.87	2.11	0.11
	1000-10000	66	1.26	0.97	0.69	22.46	5.13	0.20
	10000-100000	34	1.26	0.97	0.80	43.77	10.43	0.42
	>100000	7	1.07	1.02	0.98	48.09	25.02	3.18
Nelson	10-100	4	0.67	0.47	0.31	2.73	0.95	0.31
	100-1000	36	1.02	0.62	0.32	10.82	1.85	0.07
	1000-10000	51	1.54	0.76	0.34	13.17	2.01	0.06
	10000-100000	9	1.22	1.01	0.88	3.79	1.89	0.79
St John	1000-10000	5	0.86	0.66	0.50	8.57	4.90	2.67
	10000-100000	1	0.87	0.87	0.87	20.90	20.90	20.90
St Lawrence	10-100	5	0.76	0.45	0.28	1.62	0.84	0.45
	100-1000	40	0.99	0.65	0.28	7.98	2.19	0.33
	1000-10000	37	0.94	0.78	0.47	10.25	3.88	0.37
	10000-100000	4	1.01	0.91	0.87	18.86	11.48	6.83
Yukon	100-1000	2	0.94	0.94	0.94	3.16	2.42	1.68
	1000-10000	15	1.37	0.99	0.90	11.81	3.16	0.20
	10000-100000	8	1.05	0.92	0.82	25.33	14.84	6.57
	>100000	2	1.09	1.05	1.02	32.89	24.66	16.92

Supplementary Material

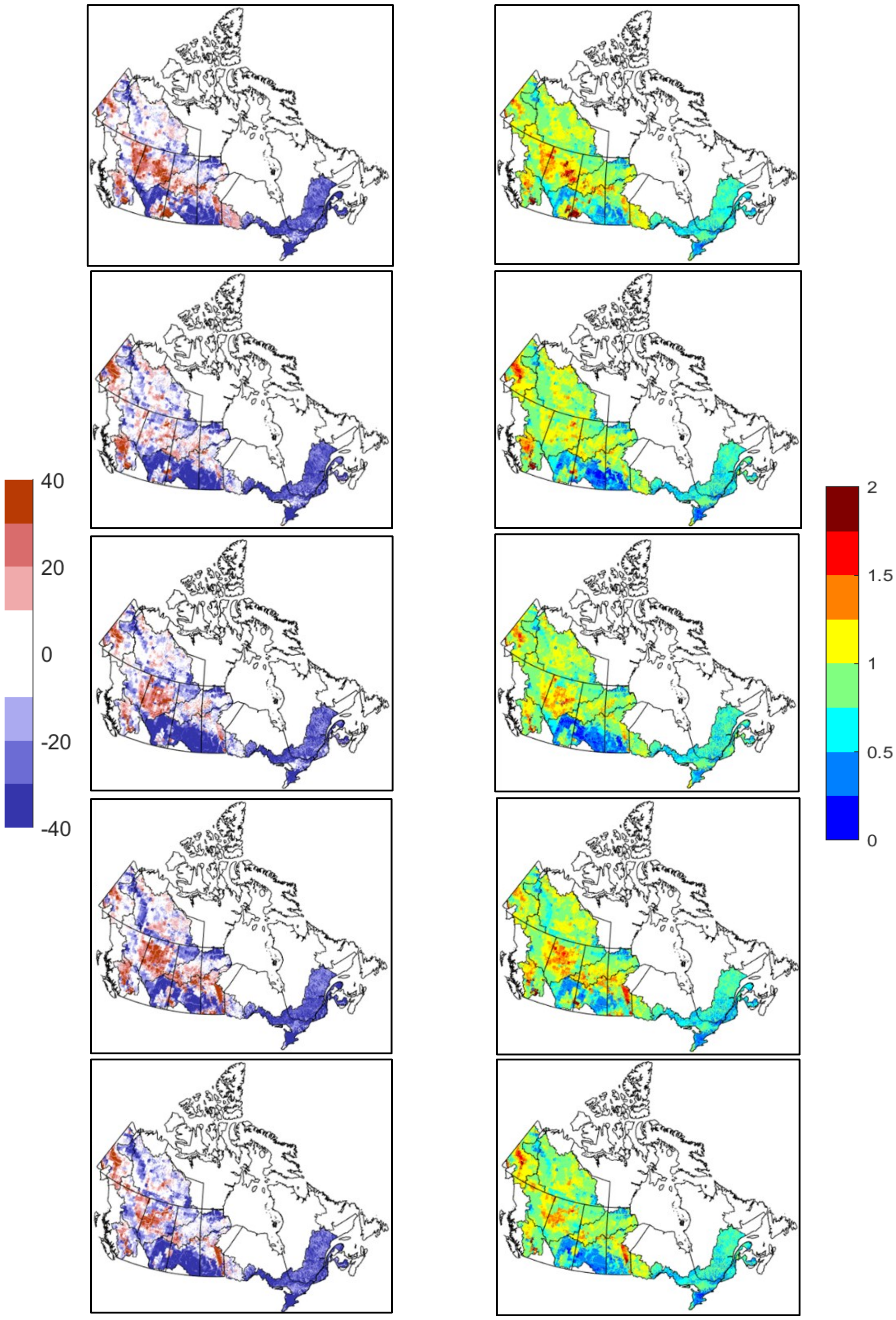

Figure S1 Projected changes to 75-year design flood (in percentage) for the study region (left panel) and the respective calculated value for the ratio R_C (right panel) for each of the five members in the ensemble using approach 2.

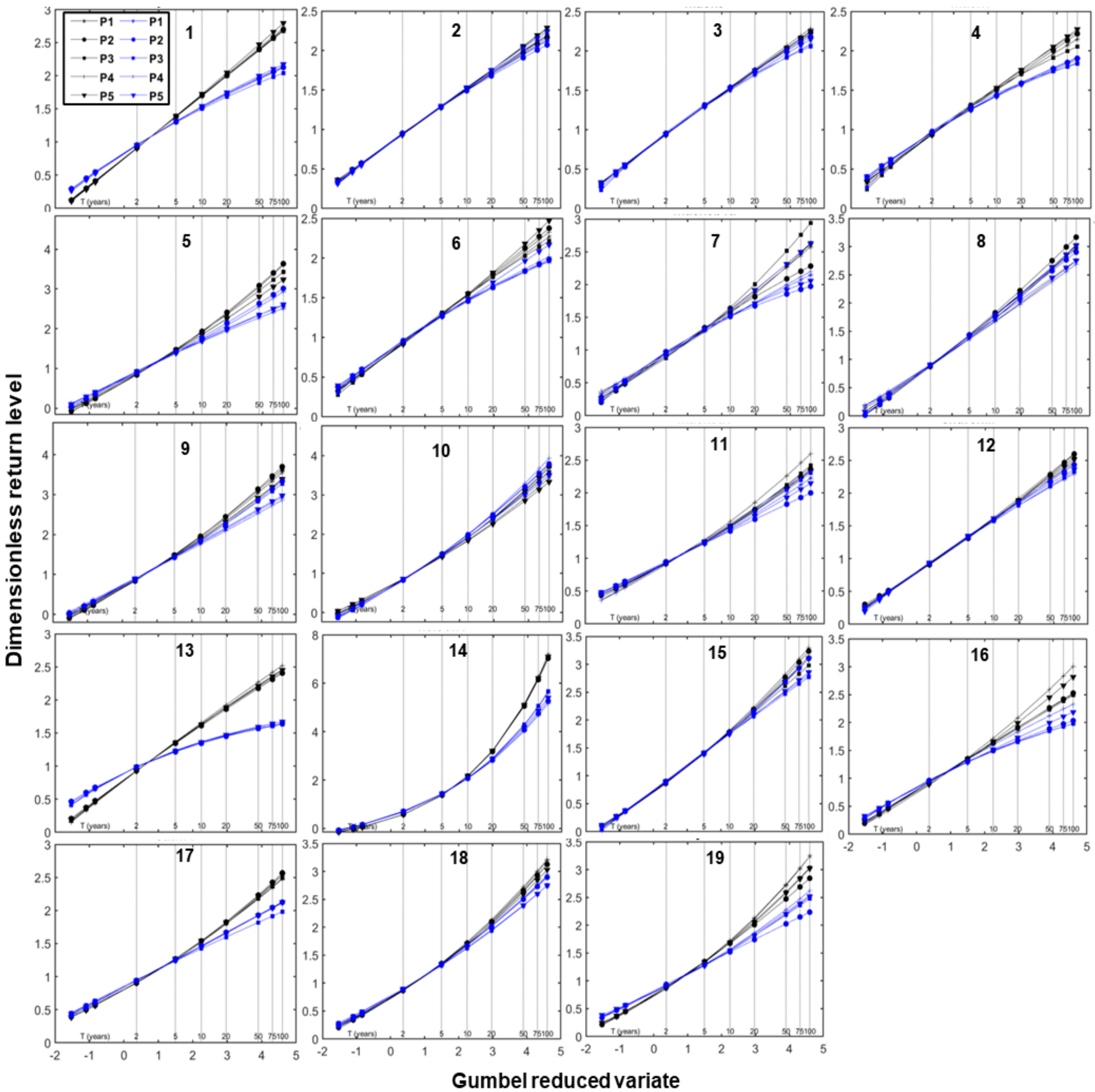

Figure S2 Regional growth curves derived for each member of the ensemble for the current time period, using RFA approach 1(in blue) and approach 2 (in black) for the 19 study regions (see Figure 1; 1: Yukon, 2–11: Sub-basins of Mackenzie, 12: Churchill , 13: Fraser , 14–16: Nelson, 17–18: St Lawrence, 19: St John).

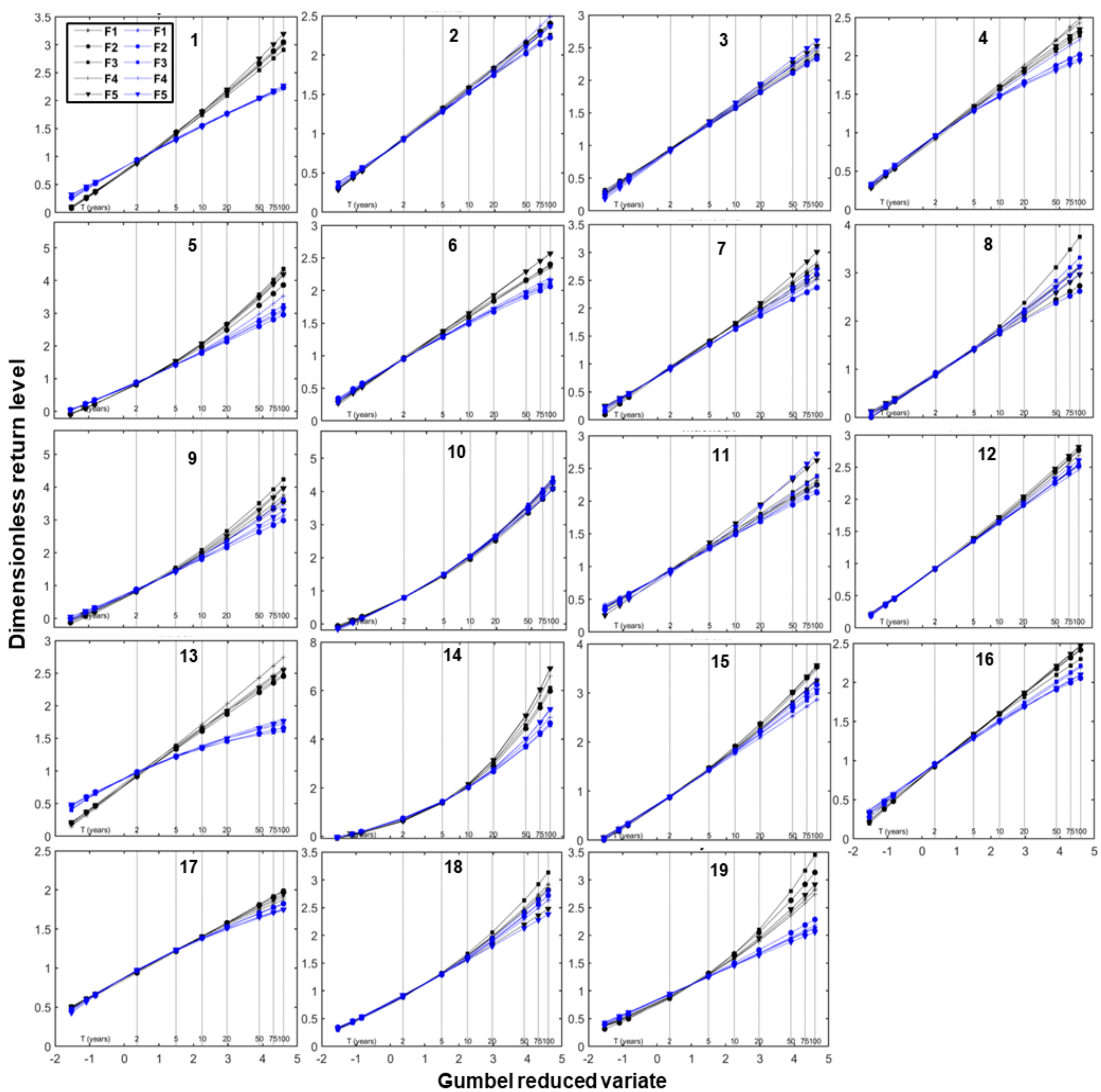

Figure S3 Regional growth curves derived for each member of the ensemble for the future time period, using RFA approach 1(in blue) and approach 2 (in black) for the 19 study regions (see Figure 1; 1: Yukon, 2–11: Sub-basins of Mackenzie, 12: Churchill , 13: Fraser , 14–16: Nelson, 17–18: St Lawrence, 19: St John).

CHAPTER 4 – DISCUSSION

This chapter provides additional discussion on the main assumptions and limitations of this study. Canada's diverse topography and climatic conditions makes its difficult for a unified approach in flood estimation and in the view of a changing climate it is essential to develop a framework to incorporate the projected changes to design considerations for various regions. This study proposes such a framework that can be adapted and integrated into existing methods in the form of changes to Creager's equation for peak flood estimation. The application of this framework in the Canadian context suggests varying correction factors to Creager curve across different regions in Canada, indicating different vulnerabilities.

4.1 Assumptions and Limitations

The assumptions utilized in the simulation and the subsequent analysis undertaken in this study are discussed below. This study utilizes a five-member ensemble of streamflow simulations at 5 km resolution performed using a cell-to-cell routing scheme, WATROUTE, driven by surface runoff and drainage from an ensemble of 50 km resolution Global Environmental Multiscale (GEM) simulations. Details of the routing scheme is presented here. The routing scheme solves the water balance equation at each grid cell and relates channel water storage to outflow from the grid cell, using Manning's equation. The water balance equation is as follows:

$$\frac{dS}{dt} = I - Q(S), \tag{20}$$

where S is the channel storage (m^3), t is time (s), I is the inflow rate (m^3/s), and Q(S) is the outflow rate (m^3/s). The equation relating channel storage to streamflow, applying Manning's equation, is:

$$Q = \frac{1}{n_k}\left(\frac{S}{L}\right)^{4/3}\tilde{s}^{1/2}, \tag{21}$$

where $\tilde{s}$ and L are respectively the slope (m/m), and length of the stream segment (m), and n_k a combined roughness parameter (s/[$m^{1/3}$]). In WATROUTE, bank full storage is determined using the following geomorphological relation between drainage area and cross-section area:

$$A_{BF} = a + bA_{DRAIN}^{c} \tag{22}$$

where A_{DRAIN} is the upstream drainage area (km^2) and a, b, and c are constants, which can be empirically derived by measuring the characteristics specific to each watercourse. When storage (S) exceeds bank full storage ($S_{BF}=A_{BF}L$), the equation solved by WATROUTE is:

$$Q = \frac{\tilde{s}^{\frac{1}{2}}}{L^{\frac{4}{3}}}\left(\frac{S_{BF}^{\frac{4}{3}}}{n_k} + \frac{(S - S_{BF})^{\frac{4}{3}}}{n_{ob}}\right) \tag{23}$$

where ($S_{BF}=A_{BF}L$) is the bank full storage (m^3), and n_{ob} is the overbank roughness coefficient. The flow directions, river lengths, and slopes required by the routing scheme are derived from the HydroSHEDS database, available at 30-arcsecond spatial resolution, following the upscaling method employed by Huziy and Sushama (2013).

As mentioned earlier, the study uses a 5 km resolution simulation. The relatively coarse resolution may not accurately capture the precise magnitude of streamflow introducing potential errors, since it does not take into account the surface heterogeneity and soil characteristics. Although the model validation was conducted in Teufel & Sushama (2021) and demonstrated reasonable accuracy in capturing magnitude, timing, and variability across most regions, it was observed that the model underestimates peak flow by 30% in some regions. Figure 4.1 shows the mean annual maximum daily streamflow at 5 km resolution for the 1981–2010 period from the ERA-Interim simulation (validation simulation) and corresponding observational data from valid HYDAT stations. Similar to the results in Teufel & Sushama (2021), the model captures the magnitude and pattern reasonably. However, underestimation in values can be observed, especially in the southern regions. These biases can be improved by using higher resolution models or by using multiple models. This study assumes that any biases are present in both present and future simulations considered and would cancel out when assessing the climate change signal. Hence the ratio is presumed to sufficiently capture the projected changes without significant errors.

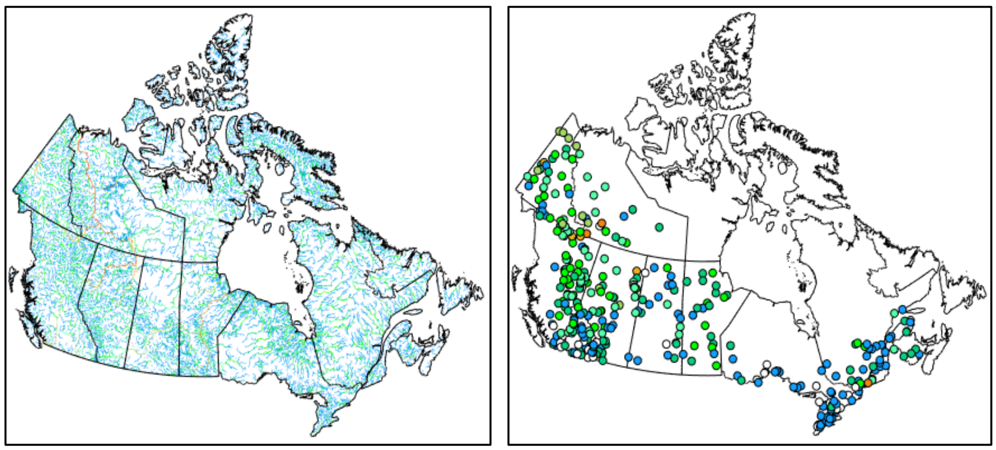

(a)

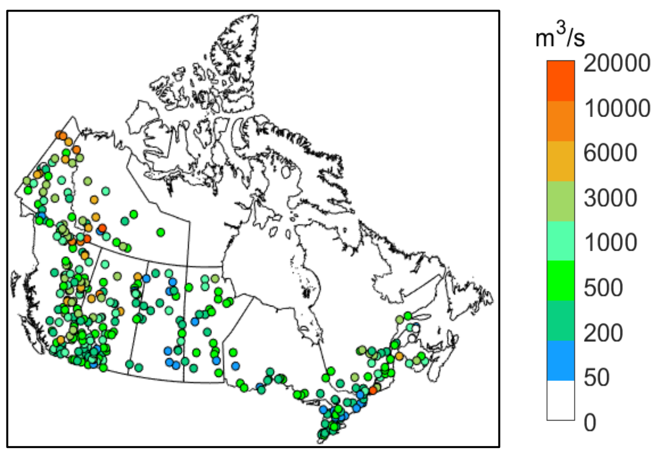

(b)

Figure 4.1 (a) Mean Annual Maximum daily streamflow in ERA-Interim for 1981-2010 period (left panel) and the respective values at valid station points (right panel) (b) Mean Annual Maximum daily streamflow at valid HYDAT stations for 1981–2010 period.

The Creager's coefficient (*C)* calculated using the maximum mean daily flows, as mentioned previously, are lower than the instantaneous flow at the site. As a result, the Creager curves constructed using instantaneous flow would probably yield higher *C* values compared to the results presented in this study. However, the future alterations in mean daily flood and instantaneous floods will be proportional, and the derived ratio can be presumed to effectively encapsulate the nature of these anticipated changes also.

Some of the identified limitations of this study is discussed in the following paragraphs. The variability in climate, coupled with the dynamic nature of land use, requires sophisticated statistical methods like cluster analysis to effectively categorize regions, this study however uses objective partitioning based on climatic zones to group sites into regions for FFA. The homogenous regions derived does not completely satisfy the homogeneity criteria set by Hosking & Wallis (1997) and could be further divided but was not considered given limited observations. A focused study on a smaller region could provide more accurate results with inclusion of more data points and ensuring that the smaller regions satisfy the homogeneity measures or using statistical methods to pool data from multiple regions to arrive at flood quantiles using methods like cluster analysis. Such a detailed study would give more accurate results especially when constructing Creager curves using historical data. The lack of observational data can be over come by developing streamflow through hydrological modelling or using machine learning algorithms (Javelle et al., 2002; Ohnishi et al., 2004; Gizaw & Gan, 2016; Rouhani & Leconte, 2018; Carmo et al., 2024).

The study also assumes the same statistically homogeneous regions for the second approach. This larger dataset can also be used to devise a different set of homogenous regions that can be used for analysis in the second phase of the framework, however this was not considered in this study.

Frequency analysis in this study relies on the assumption of stationarity. However, given the extended data period, it is worthwhile undertaking non-stationarity analysis (Tan & Gan, 2015; Shrestha et al., 2017; Wang et al., 2021). This study's conclusions rely on a single RCM simulation and the RCP 8.5 emission scenario. To address uncertainties associated with models and emission scenarios, it is essential to incorporate additional models and diverse emission scenarios when updating the Creager curves.

4.2 Implications and future research

The correction factors in most regions where this framework is applied for Canada suggest a projected increase in floods in future. The ratio when applied to existing Creager curves will change the envelope to account for the projected increase in flood. As a result, structures that have been constructed in accordance with the existing guidelines will need to be re-evaluated to ensure compliance with the updated standards. This underscores the importance of adapting infrastructure and design practices to address changing hydrological conditions and flood characteristics and minimize potential future risks.

The results of this study can be further improved by incorporating findings from multiple models and emission scenarios to assess the projected changes and by using hydrological or machine learning approaches to estimate flood at ungauged stations to develop Creager curves. This refinement can occur at smaller scales, such as watershed or provincial levels, allowing for the formulation of guidelines that can be seamlessly integrated into design codes. Higher resolution models will be able to capture the flood generating mechanisms in more detail and accuracy, adding more value.

In this study, the primary focus is on adapting the design floods for highway bridges that traverse rivers, specifically utilizing Creager curves for the 75-year flood. However, the versatility of the proposed framework allows for its extension to evaluate climate resilience for a range of structures. By analyzing different return levels, the framework can be applied to assess the impact of climate change on various types of water infrastructure beyond river-crossing highway bridges, like reservoirs, aquifers, or river training structures. Furthermore, it provides a flexible tool for evaluating corrections that may be needed for different envelope curves or equations, offering a comprehensive approach to enhancing the climate adaptation of diverse infrastructure assets. This adaptability underscores the broader applicability and utility of the framework in addressing the challenges posed by climate change across various engineering and construction contexts.

CHAPTER 5 – CONCLUSIONS AND RECOMMENDATIONS

This study introduces a comprehensive framework for updating flood envelope curves, concentrating on seven major Canadian river basins (i.e., Fraser, Nelson, Mackenzie, Yukon, Churchill, St Lawrence and St John) that collectively cover a substantial portion of the country. The initial step involves establishing Creager curves for the study regions considering 75-year design floods, derived through Regional Frequency Analysis (RFA) of annual maximum mean daily flows obtained from the HYDAT database spanning the period 1950–2020.

The correction factors (R_C) are then evaluated through two distinct approaches. These approaches use a five-member ensemble of streamflow simulations for the time period 1951–2099, generated using an integrated climate-hydrology regional climate modeling system. The first approach estimates R_C at observation sites by comparing future and current C values. Future and current design flood values are estimated using the RFA approach, focusing only on the 5 km grid cells where the observation stations are situated.

In the second approach, a similar comparison is made, but it considers all grid cells within a given region in the RFA approach to estimate future and current design flood magnitudes. This approach provides additional information in terms of increased visibility of spatial patterns and information at ungauged regions. This study provides a robust methodology for updating flood envelope curves and accommodating the complexities of future climate changes in the design flood estimation process, which would be useful to practitioners.

The main findings of this study are listed below:

- The Creager coefficient, extracted from observations, i.e., for current climate, display significant variability across the study region, ranging from less than 1 to over 40, with the Mackenzie River basin showing the highest values, around 45. This variability is attributed to variability in streamflow brought by diverse climate conditions, landforms, and geographic influences affecting flood mechanisms in different areas of the study domain.
- The ratio R_C exhibits both values above and below one across the study domain suggesting both increases and decreases in projected design flood over the study region, with approximately 24.5% of observation stations likely to have $R_C > 1$. Notably, the Churchill River basin shows $R_C > 1$ for 70% of stations, while the St. John River basin generally displays $R_C < 1$. A value greater than one indicates that the curves would need to be shifted upwards to accommodate the projected increase in design floods, whereas for regions where R_C is less than one, the design flood is not projected to increase, and the curves would not have to be modified.
- An assessment of the spread of R_C values, quantified through the coefficient of variation based on five pairs of current and future period simulations, indicates higher confidence for most parts of the study domain. However, certain regions, particularly parts of the Nelson River and St. Lawrence River basins, show lower confidence in the spread of R_C values. It is important to note that the base model providing runoff data for streamflow estimation is GEM for all five members and will therefore tend to be more similar that five different models.
- Integrating simulated streamflow data for ungauged locations by considering all grid cells within a region, proves to be an effective strategy for addressing data availability limitations, where observation stations are not present. R_C values exceeding 1 are observed

for 32.89% of grid cells, with more substantial increases in western Canada using this approach. The maximum value of R_C obtained for each region is higher than that of approach one, however, the results are comparable for the station locations considered in approach one.

Future research should explore conducting a comparable analysis, either by directly integrating model-simulated instantaneous peak flows or by converting mean daily flows to instantaneous peak flows for assessing projected changes flows using appropriate methods such as those included in Sangal (1981), Chen et al. (2017) and Khaliq (2023). Additionally, the potential of using machine learning approaches to generate data at ungauged regions for the development of envelope curves is anticipated to augment and reinforce the findings presented in this study. It is also crucial to recognize that the findings of this study are based on transient climate change simulations from a single RCM and employing a single emission scenario and to account for model and emission scenario related uncertainties, additional models and emission scenarios must be considered in the future.

REFERENCES

Abdullah, J., Muhammad, N. S., Muhammad, S. A., & Julien, P. Y. (2019). Envelope curves for the specific discharge of extreme floods in Malaysia. *Journal of Hydro-Environment Research*, *25*, 1-11. https://doi.org/10.1016/j.jher.2019.05.002

Abrahamson, B. (2010). Probable maximum flood estimator for British Columbia. Agriculture and Agri-Foods Canada. *Agri-Environment Services Branch*, 1-35.

Acreman, M., & Sinclair, C. (1986). Classification of drainage basins according to their physical characteristics; an application for flood frequency analysis in Scotland. *Journal of Hydrology*, *84*(3-4), 365-380.

Ahmadi, S. M., & Ahmadi, M. T. Hydrodynamic considerations for improving the design/evaluation of over-topped bridge decks during extreme floods. *Structure and Infrastructure Engineering*, 1-15. https://doi.org/10.1080/15732479.2023.2171069

Ahsan, H., Nabi, G., Boota, M. W., & Abbas, T. (2016). Development of envelope curve for Indus and Jhelum River basin in Pakistan and estimation of upper bound using envelope curve. *Journal of Himalayan Earth Science*, *49*(1).

Alberta Transportation (2007) Alberta Flood Envelope Curve Analysis.

Arora, V. K., Scinocca, J., Boer, G., Christian, J., Denman, K., Flato, G., Kharin, V., Lee, W., & Merryfield, W. (2011). Carbon emission limits required to satisfy future representative concentration pathways of greenhouse gases. *Geophysical Research Letters*, *38*(5). https://doi.org/10.1029/2010GL046270

Aucoin, F., Caissie, D., El-Jabi, N., & Turkkan, N. (2011). Flood frequency analyses for New Brunswick rivers. 0706-6457

Awasthi, C., Archfield, S. A., Ryberg, K. R., Kiang, J. E., & Sankarasubramanian, A. (2022). Projecting Flood Frequency Curves under near-term climate change. *Water Resources Research*, *58*(8), e2021WR031246. https://doi.org/10.1029/2021WR031246

Beauchamp, J., Leconte, R., Trudel, M., & Brissette, F. (2013). Estimation of the summer ‐ fall PMP and PMF of a northern watershed under a changed climate. *Water Resources Research*, *49*(6), 3852-3862. https://doi.org/10.1002/wrcr.20336

Beniston, M., Stephenson, D. B., Christensen, O. B., Ferro, C. A., Frei, C., Goyette, S., Halsnaes, K., Holt, T., Jylhä, K., & Koffi, B. (2007). Future extreme events in European climate: an exploration of regional climate model projections. *Climatic Change*, *81*, 71-95. http://dx.doi.org/10.1007/s10584-006-9226-z

Bertola, M., Blöschl, G., Bohac, M., Borga, M., Castellarin, A., Chirico, G. B., Claps, P., Dallan, E., Danilovich, I., & Ganora, D. (2023). Megafloods in Europe can be anticipated from observations in hydrologically similar catchments. *Nature geoscience*, *16*(11), 982-988. https://doi.org/10.1038/s41561-023-01300-5

Bhatkoti, R., Moglen, G. E., Murray-Tuite, P. M., & Triantis, K. P. (2016). Changes to bridge flood risk under climate change. *Journal of Hydrologic Engineering*, *21*(12), 04016045.

Bonsal, B. R., Peters, D. L., Seglenieks, F., Rivera, A., & Berg, A. (2019). Changes in freshwater availability across Canada. *Canada's changing climate report*, 261-342.

Burn, D. H. (1990). Evaluation of regional flood frequency analysis with a region of influence approach. *Water Resources Research*, *26*(10), 2257-2265.

Bush, E. and Lemmen, D.S.(2019) Canada's Changing Climate Report. Government of Canada, Ottawa, ON. 444 p.

Buttle, J. M., Allen, D. M., Caissie, D., Davison, B., Hayashi, M., Peters, D. L., Pomeroy, J. W., Simonovic, S., St-Hilaire, A., & Whitfield, P. H. (2016). Flood processes in Canada: Regional and special aspects. *Canadian Water Resources Journal / Revue canadienne des ressources hydriques*, *41*(1-2), 7-30. https://doi.org/10.1080/07011784.2015.1131629

Carmo, F. C. P. d., John, J., Sushama, L., & Khaliq, M. N. (2024). Deep Learning Modeling Framework for Multi-Resolution Streamflow Generation. *Journal of Water and Climate Change*. (Accepted)

Castellarin, A. (2007). Probabilistic envelope curves for design flood estimation at ungauged sites. *Water Resources Research*, *43*(4).

Castellarin, A., Vogel, R. M., & Matalas, N. C. (2005). Probabilistic behavior of a regional envelope curve. *Water Resources Research*, *41*(6). https://doi.org/10.1029/2004WR003042

Chaves, L. G., Studart, T. M. d. C., Campos, J. N. B., & Souza, F. A. d. (2017). Regional envelope curves for the state of Ceará: a tool for verification of hydrological dam safety. *RBRH*, *22*. https://doi.org/10.1590/2318-0331.021720160062

Chen, B., Krajewski, W. F., Liu, F., Fang, W., & Xu, Z. (2017). Estimating instantaneous peak flow from mean daily flow. *Hydrology Research*, *48*(6), 1474-1488. https://doi.org/10.2166/nh.2017.200

Clavet-Gaumont, J., Huard, D., Frigon, A., Koenig, K., Slota, P., Rousseau, A., Klein, I., Thiémonge, N., Houdré, F., & Perdikaris, J. (2017). Probable maximum flood in a changing climate: An overview for Canadian basins. *Journal of Hydrology: Regional Studies*, *13*, 11-25. https://doi.org/10.1016/j.ejrh.2017.07.003

Clavet‐Gaumont, J., Sushama, L., Khaliq, M., Huziy, O., & Roy, R. (2013). Canadian RCM projected changes to high flows for Québec watersheds using regional frequency analysis. *International journal of climatology*, *33*(14), 2940-2955. https://doi.org/10.1002/joc.3641

Coles, S., Bawa, J., Trenner, L., & Dorazio, P. (2001). An Introduction to Statistical Modeling of Extreme Values. *208*.

*Core Basins and Observatories - Global Water Futures.*University of Saskatchewan. Retrieved 25 February from https://gwf.usask.ca/projects-facilities

Côté, J., Gravel, S., Méthot, A., Patoine, A., Roch, M., & Staniforth, A. (1998). The operational CMC–MRB global environmental multiscale (GEM) model. Part I: Design considerations and formulation. *Monthly Weather Review*, *126*(6), 1373-1395. https://doi.org/10.1175/1520-0493(1998)126%3C1373:TOCMGE%3E2.0.CO;2

Coulbourne, W. L., Kriebel, D. L., Behm, R. L., & McKenna, K. K. (2021). *Guide for design of flood-resistant buildings*. 265 https://doi.org/10.4224/40002704

Creager, W. P., Justin, J. D., & Hinds, J. (1945). Engineering for Dams. v.1.

Crippen, J. R. (1982). Envelope curves for extreme flood events. *Journal of the Hydraulics Division*, *108*(10), 1208-1212. https://doi.org/10.1061/JYCEAJ.0005916

Crippen, J. R., & Bue, C. D. (1977). *Maximum floodflows in the conterminous United States* (Vol. 1887). US Government Printing Office.

Dalrymple, T. (1960). Flood-Frequency Analyses, Manual of Hydrology: Part 3. https://doi.org/10.3133/wsp1543A

Darch, G. J. C., & Jones, P. D. (2012). Design flood flows with climate change: method and limitations. Proceedings of the Institution of Civil Engineers-Water Management,

Das, T., Dettinger, M. D., Cayan, D. R., & Hidalgo, H. G. (2011). Potential increase in floods in California's Sierra Nevada under future climate projections. *Climatic Change*, *109*, 71-94.

Dawson, R., Thompson, D., Johns, D., Gosling, S., Chapman, L., Darch, G., Watson, G., Powrie, W., Bell, S., & Paulson, K. (2016). Infrastructure. *UK climate change risk assessment evidence report.* 226 p.

DeCoursey, D. G. (1973). "Objective regionalization of peak flow rates, in flood and droughts." *Proc., 2nd Int. Symp. in Hydrology*, E. F. Koelzer and K. Mahmood, eds., Water Resources Publications, Fort Collins, CO, 395–405.

Devendiran, D. K., Banerjee, S., & Mondal, A. (2021). Impact of climate change on multihazard performance of river-crossing bridges: Risk, resilience, and adaptation. *Journal of Performance of Constructed Facilities*, *35*(1), 04020127.

du Plessis, J., & Masule, S. (2023). Revised Regional Maximum Flood (RMF) method and regionalisation. *Journal of the South African Institution of Civil Engineering*, *65*(3), 2-19. http://dx.doi.org/10.17159/2309-8775/2023/v65n3a1

ECCC (Environment and Climate Change Canada) (2023). *Environment and Climate Change Canada - Climate Trends and Variations Bulletin* https://www.canada.ca/en/environment-climate-change/spring-2023-bulletin.html

Ewea, H. A., Al-Amri, N. S., & Elfeki, A. M. (2020). Analysis of maximum flood records in the arid environment of Saudi Arabia. *Geomatics, Natural Hazards and Risk*, *11*(1), 1743-1759. https://doi.org/10.1080/19475705.2020.1810783

Faulkner, D., Warren, S., & Burn, D. (2016). Design floods for all of Canada. *Canadian Water Resources Journal/Revue Canadienne Des Ressources Hydriques*, *41*(3), 398-411. https://doi.org/10.1080/07011784.2016.1141665

Fowler, H., & Ekström, M. (2009). Multi‐model ensemble estimates of climate change impacts on UK seasonal precipitation extremes. *International Journal of Climatology: A Journal of the Royal Meteorological Society*, *29*(3), 385-416. https://doi.org/10.1002/joc.1827

François, B., Schlef, K., Wi, S., & Brown, C. (2019). Design considerations for riverine floods in a changing climate–a review. *Journal of Hydrology*, *574*, 557-573. https://doi.org/10.1016/j.jhydrol.2019.04.068

Francou, J., & Rodier, J. (1967). Essai de classification des crues maximales observées dans le monde. ORSTOM.

Gado, T. A., & Nguyen, V.-T.-V. (2016). Comparison of homogenous region delineation approaches for regional flood frequency analysis at ungauged sites. *Journal of Hydrologic Engineering*, *21*(3), 04015068.

Gingras, D., Adamowski, K., & Pilon, P. J. (1994). Regional flood equations for the provinces of Ontario and Quebec 1. *JAWRA Journal of the American Water Resources Association*, *30*(1), 55-67.

Gizaw, M. S., & Gan, T. Y. (2016). Regional flood frequency analysis using support vector regression under historical and future climate. *Journal of Hydrology*, *538*, 387-398.

Guide to Bridge Hydraulics. https://doi.org/10.1680/gtbh2e.32620

Habeeb, B., & Bastidas-Arteaga, E. (2023). Assessment of the impact of climate change and flooding on bridges and surrounding area. *Frontiers in Built Environment*, *9*, 1268304. https://doi.org/10.3389/fbuil.2023.1268304

Hay, L. E., Wilby, R. L., & Leavesley, G. H. (2000). A comparison of delta change and downscaled GCM scenarios for three mountainous basins in the United States 1. *JAWRA Journal of the American Water Resources Association*, *36*(2), 387-397. https://doi.org/10.1111/j.1752-1688.2000.tb04276.x

Helsel, D. R., Hirsch, R. M., Ryberg, K. R., Archfield, S. A., & Gilroy, E. J. (2020). Statistical methods in water resources. *Techniques and Methods*, 484

Hosking, J. R. M., & Wallis, J. R. (1997). Regional Frequency Analysis. 238.

Huziy, O., Sushama, L., Khaliq, M., Laprise, R., Lehner, B., & Roy, R. (2013). Analysis of streamflow characteristics over Northeastern Canada in a changing climate. *Climate dynamics*, *40*, 1879-1901. https://doi.org/10.1007/s00382-012-1406-0

IPCC. (2023). Sections. In: Climate Change 2023: Synthesis Report. Contribution of Working Groups I, II and III to the Sixth Assessment Report of the Intergovernmental Panel on Climate Change [Core Writing Team, H. Lee and J. Romero (eds.)]. 35-115. https://doi.org/10.59327/IPCC/AR6-9789291691647

Jarvis, C. (1926). Flood flow characteristics. *Transactions of the American Society of Civil Engineers*, *89*(1), 985-1032.

Javelle, P., Ouarda, T. B., Lang, M., Bobée, B., Galéa, G., & Grésillon, J.-M. (2002). Development of regional flood-duration–frequency curves based on the index-flood method. *Journal of Hydrology*, *258*(1-4), 249-259. https://doi.org/10.1016/S0022-1694(01)00577-7

Jeong, D. I., Sushama, L., Khaliq, M. N., & Roy, R. (2014). A copula-based multivariate analysis of Canadian RCM projected changes to flood characteristics for northeastern Canada. *Climate dynamics*, *42*, 2045-2066. https://doi.org/10.1007/s00382-013-1851-4

Kashinath, K., Mustafa, M., Albert, A., Wu, J., Jiang, C., Esmaeilzadeh, S., Azizzadenesheli, K., Wang, R., Chattopadhyay, A., & Singh, A. (2021). Physics-informed machine learning: case studies for weather and climate modelling. *Philosophical Transactions of the Royal Society A*, *379*(2194), 20200093. https://doi.org/10.1098/rsta.2020.0093

Khaliq, M., Sushama, L., Monette, A., & Wheater, H. (2015). Seasonal and extreme precipitation characteristics for the watersheds of the Canadian Prairie Provinces as simulated by the NARCCAP multi-RCM ensemble. *Climate dynamics*, *44*, 255-277. https://doi.org/10.1007/s00382-014-2235-0

Khaliq, M. N. (2019). *An inventory of methods for estimating climate change-informed design water levels for floodplain mapping* (978-0-660-30536-3). (Technical Report (National Research Council of Canada. Ocean, Coastal and River Engineering); no. NRC-OCRE-2019-TR-011, Issue.

Khaliq, M. N. (2023). Estimation of instantaneous peak flows in Atlantic Canada. *Annual Conference of the Canadian Society for Civil Engineering*.

Kouwen, N., Soulis, E. D., Pietroniro, A., Donald, J., & Harrington, R. A. (1993). Grouped response units for distributed hydrologic modeling. *Journal of Water Resources Planning and Management*, *119*(3), 289-305. https://doi.org/10.1061/(ASCE)0733-9496(1993)119:3(289)

Kumar, R. (2023) Design flood estimation for flood disaster Resilient bridges exposed to climate change, EGU General Assembly 2023, Vienna, Austria, 24–28 Apr 2023, EGU23-882, https://doi.org/10.5194/egusphere-egu23-882

Kundzewicz, Z. W., & Licznar, P. (2021). Climate change adjustments in engineering design standards: European perspective. *Water Policy*, *23*(S1), 85-105. https://doi.org/10.2166/wp.2021.330

Kwon, H.-H., Sivakumar, B., Moon, Y.-I., & Kim, B.-S. (2011). Assessment of change in design flood frequency under climate change using a multivariate downscaling model and a precipitation-runoff model. *Stochastic Environmental Research and Risk Assessment*, *25*, 567-581. https://doi.org/10.1007/s00477-010-0422-z

Labonté-Raymond, P.-L., Pabst, T., Bussière, B., & Bresson, É. (2020). Impact of climate change on extreme rainfall events and surface water management at mine waste storage facilities. *Journal of Hydrology*, *590*, 125383.

Lehner, B., Verdin, K., & Jarvis, A. (2008). New global hydrography derived from spaceborne elevation data. *Eos, Transactions American Geophysical Union*, *89*(10), 93-94. https://doi.org/10.1029/2008EO100001

Lettenmaier, D. P., Wallis, J. R., & Wood, E. F. (1987). Effect of regional heterogeneity on flood frequency estimation. *Water Resources Research*, *23*(2), 313-323. https://doi.org/10.1029/WR023i002p00313

Lima, G. d., Marcellini, S. S., Neill, C. R., & Salla, M. R. (2017). Preliminary estimate of floods discharge in Brazil using Creager envelope curves. *RBRH*, *22*, e46.

Maidment, D. R. (1993). Handbook of Hydrology.

Mailhot, A., Lachance-Cloutier, S., Talbot, G., & Favre, A.-C. (2013). Regional estimates of intense rainfall based on the Peak-Over-Threshold (POT) approach. *Journal of Hydrology*, *476*, 188-199.

Matthai, H. F. (1969). *Floods of June 1965 in South Platte River basin, Colorado* (Water Supply Paper, Issue. U.S. Govt. Print. Off.

Meyer, M. D., & Weigel, B. (2011). Climate change and transportation engineering: Preparing for a sustainable future. *Journal of Transportation Engineering*, *137*(6), 393-403.

Mladjic, B., Sushama, L., Khaliq, M., Laprise, R., Caya, D., & Roy, R. (2011). Canadian RCM projected changes to extreme precipitation characteristics over Canada. *Journal of climate*, *24*(10), 2565-2584. https://doi.org/10.1175/2010JCLI3937.1

MNRF. (2014). Flood Flow Statistics for the Great Lakes Watershed System.

Mondoro, A., Frangopol, D. M., & Liu, L. (2018). Bridge adaptation and management under climate change uncertainties: A review. *Natural Hazards Review*, *19*(1), 04017023.

Mostofi Zadeh, S., & Burn, D. H. (2019). A super region approach to improve pooled flood frequency analysis. *Canadian Water Resources Journal/Revue Canadienne Des Ressources Hydriques*, *44*(2), 146-159.

Murphy, E., Pilechi, V., Barrette, P., Khaliq, M., & Almansour, H. (2018). Review of bridge design practice for water loads, scour, and ice action: Opportunities for climate resilience. Proc., CSCE Annual Conference

Neill, C. R. (1986). Unusual canadian floods and the creager diagram. *Canadian Journal of Civil Engineering*, *13*(2), 255-257. https://doi.org/10.1139/l86-034

Ohnishi, R., Kato, T., Imaizumi, M., & Tanji, H. (2004). A study to determine an equation of enveloping curve for regional flood peaks by maximum rainfall data. *Paddy and Water Environment*, *2*, 83-90.

Othman, H., Hussian, L., & Amleh, L. (2019). Effect of climate change on Canadian bridge infrastructures. CSCE Annual Conference, June 12-15

PaiMazumder, D., & Done, J. M. (2014). Uncertainties in long-term drought characteristics over the Canadian Prairie provinces, as simulated by the Canadian RCM. *Climate Research*, *58*(3), 209-220. https://doi.org/10.3354/cr01196

Picketts, I. M., Andrey, J., Matthews, L., Déry, S. J., & Tighe, S. (2016). Climate change adaptation strategies for transportation infrastructure in Prince George, Canada. *Regional environmental change*, *16*, 1109-1120.

Pilon, P., Alila, Y., & Adamowski, K. (1991). Assessment of risk of flooding based on regional information. *Proceedings of NATO ASI (Advanced Study Institute) on Risk and Reliability in Water Resources and Environmental Engineering*, 18-28.

Pilon, P. J., & Adamowski, K. (1992). The value of regional information to flood frequency analysis using the method of L-moments. *Canadian Journal of Civil Engineering*, *19*(1), 137-147.

Plummer, D., Caya, D., Frigon, A., Côté, H., Giguère, M., Paquin, D., Biner, S., Harvey, R., & De Elia, R. (2006). Climate and climate change over North America as simulated by the Canadian RCM. *Journal of climate*, *19*(13), 3112-3132. https://doi.org/10.1175/JCLI3769.1

Poitras, V., Sushama, L., Seglenieks, F., Khaliq, M., & Soulis, E. (2011). Projected changes to streamflow characteristics over western Canada as simulated by the Canadian RCM. *Journal of Hydrometeorology*, *12*(6), 1395-1413. https://doi.org/10.1175/JHM-D-10-05002.1

Qian, B., Jing, Q., Smith, W., Grant, B., Cannon, A. J., & Zhang, X. (2020). Quantifying the uncertainty introduced by internal climate variability in projections of Canadian crop production. *Environmental Research Letters*, *15*(7), 074032. https://doi.org/10.1088/1748-9326/ab88fc

Quintero, F., Mantilla, R., Anderson, C., Claman, D., & Krajewski, W. (2018). Assessment of changes in flood frequency due to the effects of climate change: Implications for engineering design. *Hydrology*, *5*(1), 19. https://doi.org/10.3390/hydrology5010019

Robson, A., & Reed, D. (1999). Flood Estimation Handbook: Statistical Procedures for Flood Frequency Estimation. *Institute of Hydrology, Wallingford*

Rouhani, H., & Leconte, R. (2018). A methodological framework to assess PMP and PMF in snow-dominated watersheds under changing climate conditions–A case study of three watersheds in Québec (Canada). *Journal of Hydrology*, *561*, 796-809.

Saharia, M., Kirstetter, P.-E., Vergara, H., Gourley, J. J., & Hong, Y. (2017). Characterization of floods in the United States. *Journal of Hydrology*, *548*, 524-535. https://doi.org/10.1016/j.jhydrol.2017.03.010

Sangal, B. (1981). A practical method of estimating peak from mean daily flows with application to streams in Ontario. *National Hydrology Research Institute NHRI Paper*(16).

Scaife, A. D. (2023). Improve predictive maintenance through the application of artificial intelligence: A systematic review. *Results in Engineering*, 101645. https://doi.org/10.1016/j.rineng.2023.101645

Shrestha, R. R., Cannon, A. J., Schnorbus, M. A., & Zwiers, F. W. (2017). Projecting future nonstationary extreme streamflow for the Fraser River, Canada. *Climatic Change*, *145*, 289-303.

Smith, A., Sampson, C., & Bates, P. (2015). Regional flood frequency analysis at the global scale. *Water Resources Research*, *51*(1), 539-553.

Smith, C. (1993). Selection of design flood frequencies for hydraulic structures. *Canadian Journal of Civil Engineering*, *20*(4), 582-586. https://doi.org/10.1139/l93-075

Smithers, J., & Schulze, R. (2001). Design runoff estimation: A review with reference to practices in South Africa. Proc. Tenth South Africa National Hydrology Symposium, 26–28 September 2001

Soulis, E. D., Snelgrove, K. R., Kouwen, N., Seglenieks, F., & Verseghy, D. L. (2000). Towards closing the vertical water balance in Canadian atmospheric models: coupling of the land surface scheme CLASS with the distributed hydrological model WATFLOOD. *Atmosphere-ocean*, *38*(1), 251-269. https://doi.org/10.1080/07055900.2000.9649648

St‐Jacques, J. M., Andreichuk, Y., Sauchyn, D. J., & Barrow, E. (2018). Projecting Canadian Prairie runoff for 2041‐2070 with North American regional climate change assessment program (NARCCAP) data. *JAWRA Journal of the American Water Resources Association*, *54*(3), 660-675. https://doi.org/10.1111/1752-1688.12642

Sushama, L., Laprise, R., Caya, D., Frigon, A., & Slivitzky, M. (2006). Canadian RCM projected climate‐change signal and its sensitivity to model errors. *International Journal of Climatology: A Journal of the Royal Meteorological Society*, *26*(15), 2141-2159. https://doi.org/10.1002/joc.1362

Tan, X., & Gan, T. Y. (2015). Nonstationary analysis of annual maximum streamflow of Canada. *Journal of climate*, *28*(5), 1788-1805.

Tasker, G. D. (1982). Comparing methods of hydrologic regionalization 1. *JAWRA Journal of the American Water Resources Association*, *18*(6), 965-970.

Teufel, B., & Sushama, L. (2021). 2° C vs. High Warming: Transitions to Flood-Generating Mechanisms across Canada. *Water*, *13*(11), 1494. https://doi.org/10.3390/w13111494

Teufel, B., & Sushama, L. (2022). High-resolution modelling of climatic hazards relevant for Canada's northern transportation sector. *Climate dynamics*, *59*(9-10), 3135-3151. https://doi.org/10.1007/s00382-022-06265-6

Tofiq, F., & Güven, A. (2015). Potential changes in inflow design flood under future climate projections for Darbandikhan Dam. *Journal of Hydrology*, *528*, 45-51. https://doi.org/10.1016/j.jhydrol.2015.06.023

Vadyala, S. R., Betgeri, S. N., Matthews, J. C., & Matthews, E. (2022). A review of physics-based machine learning in civil engineering. *Results in Engineering*, *13*, 100316. https://doi.org/10.1016/j.rineng.2021.100316

Wang, F., Huang, G., Cheng, G., & Li, Y. (2021). Impacts of climate variations on non-stationarity of streamflow over Canada. *Environmental Research*, *197*, 111118.

Wasko, C., Westra, S., Nathan, R., Orr, H. G., Villarini, G., Villalobos Herrera, R., & Fowler, H. J. (2021). Incorporating climate change in flood estimation guidance. *Philosophical Transactions of the Royal Society A*, *379*(2195), 20190548. https://doi.org/10.1098/rsta.2019.0548

Watt, W. E. (1989). Hydrology of floods in Canada - a Guide to Planning and Design. *National Research Council Canada, Ottawa, Canada*, 263.

Wiltshire, S. (1986). Regional flood frequency analysis I: Homogeneity statistics. *Hydrological Sciences Journal*, *31*(3), 321-333. https://doi.org/10.1080/02626668609491051

Yang, L. (2016). *Regional flood frequency analysis for Newfoundland and Labrador using the L-Moments index-flood method* (Doctoral dissertation, Memorial University of Newfoundland).

Yue, S., & Wang, C. Y. (2004). Possible regional probability distribution type of Canadian annual streamflow by L-moments. *Water Resources Management*, *18*(5), 425-438. https://doi.org/10.1023/B:WARM.0000049145.37577.87

Zhang, Z., & Stadnyk, T. A. (2020). Investigation of attributes for identifying homogeneous flood regions for regional flood frequency analysis in Canada. *Water*, *12*(9), 2570.

Zhang, Z., Stadnyk, T. A., & Burn, D. H. (2020). Identification of a preferred statistical distribution for at-site flood frequency analysis in Canada. *Canadian Water Resources Journal/Revue Canadienne Des Ressources Hydriques*, *45*(1), 43-58.